J. Math. Anal. Appl. 388 (2012) 231–247

Contents lists available at SciVerse ScienceDirect

Journal of Mathematical Analysis and Applications

www.elsevier.com/locate/jmaa

# Analysis of an optimal control problem for the tridomain model in cardiac electrophysiology

Bedr'Eddine Ainseba [a], Mostafa Bendahmane [a], Ricardo Ruiz-Baier [b,*]

[a] Institut de Mathématiques de Bordeaux UMR CNRS 5251, Université Victor Segalen Bordeaux 2, F-33076 Bordeaux Cedex, France
[b] Modeling and Scientific Computing, MATHICSE, École Polytechnique Fédérale de Lausanne, CH-1015 Lausanne, Switzerland

ARTICLE INFO

*Article history:*
Received 22 September 2010
Available online 28 November 2011
Submitted by J.J. Nieto

*Keywords:*
Optimal control
Finite volume approximation
Convergence
Cardiac electrophysiology
Tridomain model

ABSTRACT

In the present paper, an optimal control problem constrained by the tridomain equations in electrocardiology is investigated. The state equations consisting in a coupled reaction–diffusion system modeling the propagation of the intracellular and extracellular electrical potentials, and ionic currents, are extended to further consider the effect of an external bathing medium. The existence and uniqueness of solution for the tridomain problem and the related control problem is assessed, and the primal and dual problems are discretized using a finite volume method which is proved to converge to the corresponding weak solution. In order to illustrate the control of the electrophysiological dynamics, we present some preliminary numerical experiments using an efficient implementation of the proposed scheme.



## 1. Introduction

### 1.1. Scope

Recently, mathematical modeling and numerical simulation has become an important support to experimental studies, for investigating the electrical activity in the heart, with a particular attention to irregular heartbeat (arrhythmias) and other cardiac anomalies. The most known and most used model in electro-cardiology is represented by the so-called bidomain equations (see e.g. [20,30]). Here we investigate a variant of that model, namely the tridomain model (see [3,12] for more details concerning this model). Comparing to the bidomain model, the tridomain model additionally takes into account the interface effects of a volume conductor such as a perfusing bath, blood or an external matrix. From the mathematical viewpoint, the model consists in a degenerate reaction–diffusion system of partial differential equations modeling the intra- and extra-cellular electric potentials of the anisotropic cardiac tissue (macroscale), coupled with an elliptic equation for the bathing medium and an ordinary differential equation, describing the cellular membrane dynamics.

In this paper we are concerned with the mathematical and numerical analysis of an optimal control problem arising in the study of certain electrophysiological phenomena in the cardiac tissue, where the tridomain model plays the role of governing state equations. Motivated by [5], we introduce herein a notion of a weak solution for the underlying state problem and prove its well-posedness. Moreover, we present a numerical scheme for this problem based on the finite volume method for the spatial discretization. We establish existence of discrete solutions to this scheme, and we show that it converges to the unique weak solution. For the analysis of our optimal control problem, we will use the so-called

* Corresponding author.
*E-mail addresses:* bedreddine.ainseba@u-bordeaux2.fr (B. Ainseba), mostafa.bendahmane@u-bordeaux2.fr (M. Bendahmane), ricardo.ruiz@epfl.ch (R. Ruiz-Baier).

0022-247X/$ – see front matter 
doi:10.1016/j.jmaa.2011.11.069

Lagrangian framework, in which the control problem is set as a constrained minimization problem. Then, if the minimum of a suitable Lagrangian functional exists, it is a stationary point.

The numerical solution of an optimal control problem constrained by PDEs requires the proper discretization of the state equations, and the treatment of an optimization problem. It is known that the order in which these stages are performed (optimizing and then discretizing, or vice versa), usually depends on the problem itself, and on the nature of the control. The choice of such order is not a minor issue, since the final results obtained with both strategies are different in general (see e.g. [19]). In our study we restrict ourselves to the *optimize-then-discretize* approach, that is, we will derive the corresponding optimality condition and then it will be discretized and solved. This approach has the advantage that the discrete adjoint system is naturally consistent with the adjoint PDE. For the optimization procedure, several strategies can be considered. Here we choose to use the nonlinear conjugate gradient method (see e.g. [33]), which is a first order optimization algorithm, since it only needs the computation of the cost functional and its gradient at each minimization step. This method is known to be robust, at least for short time horizons and functionals exhibiting a quadratic behavior in a neighborhood of the minimum. In general, the numerical treatment of optimal control problems constrained by parabolic PDEs, represents a very challenging task, provided that one needs to storage state, adjoint and control variables on every time step, and on each time step one solves an elliptic PDE system. Therefore the implementation of efficient numerical schemes and advanced computational techniques is of utmost importance.

From the standpoint of our specific application, the main goal is to determine the control response of an electrical impulse which can be able to help in e.g., low-voltage defibrillation procedures. More specifically, we are interested in determining the optimal current to be applied in the external bath, so that the peaks in the transmembrane potential are damped. In this context, it is possible to regard at the particular application of implantable Cardioverter defibrillators [21], in which the heart is paced using different sets of control parameters during a sequence of consecutive short evaluation periods, and the control can be aimed at maximizing both cardiac performance and additionally the lifetime of the device.

The control might also correspond, for instance, to a pacemaker implantation. Roughly speaking, in such procedure, a small battery-operated device (called pacemaker) is placed into the chest, to help the muscle to regularize the mechanical activity. This is a minor surgical procedure that is usually performed under local anaesthetic. The sinoatrial node is a natural pacemaker that generates the electrical impulses that drive the heartbeats. If this process stops working properly, there is a need for an artificial pacemaker. The main physiological causes are: Heart block (the heart beats more slowly or irregularly than normal), Bradycardia (the sinus node does not function properly), and heart failure (the muscle does not pumps blood efficiently enough).

To put this paper in the proper perspective, we mention that the wellposedness of the bidomain equations has been studied by several authors. Colli Franzone and Savaré [10] propose a variational formulation of the model and show after an abstract change of variable that it has a structure that fits into the framework of evolution variational inequalities in Hilbert spaces. Bendahmane and Karlsen [5] prove existence and uniqueness for the bidomain equations using the Faedo–Galerkin method and compactness theory for the existence proof. Bourgault et al. [9] proved wellposedness for the bidomain equations by first reformulating the problem into a single parabolic PDE and then applying a semigroup approach, and Veneroni [32] derives existence, uniqueness and regularity results for another formulation of the degenerate bidomain equations. From a numerical analysis point of view, several contributions have been made using finite elements methods (see [4,29,30]). In the context of finite volume approximations, we mention the works by Bendahmane et al. [6,8], where they analyze a finite volume scheme for the bidomain equations for which they proved existence, uniqueness and convergence of the numerical scheme, and the work by Coudière et al. [11], who introduce a discrete duality finite volume formulation for the heart-torso coupled problem.

Regarding the analysis of the optimal control in electrocardiology, we are only aware of the works [25,26,22] which are proposed to treat the monodomain model. In these papers, the authors present the mathematical and numerical treatment of an optimal control problem for the monodomain equations, using classical finite element methods for the spatial discretization of the problem. We recall that the monodomain model is equivalent to a scalar parabolic equation for the transmembrane potential, coupled to an ODE for the gating variable. In this nondegenerate case, an equal anisotropic ratio for the intra- and extracellular media is assumed. The recent contribution by Kunisch and Wagner [23] also includes a rigorous analysis of uniqueness and regularity of solutions for the optimal control problem related to bidomain equations. The treatment presented herein, is based on similar techniques as in Nagaiah et al. [25,26], but we here analyze a degenerate tridomain model, and we perform the spatial discretization using finite volume schemes.

The structure of the paper is organized as follows. In what is left of this section, we briefly recall the governing equations for the propagation of the electrical potential in the cardiac tissue and in the external bathing medium. Then, after providing some preliminaries and the wellposedness analysis of the forward problem (Section 2), in Section 3 we introduce the main ingredients of the corresponding optimal control problem. Next, Section 4 is concerned with the finite volume approximation of the primal problem. In Section 5 we outline the main features of the minimization gradient-based algorithm to treat the optimal control problem. Several numerical simulations are then performed to investigate the qualitative behavior of the model and proposed numerical scheme (Section 6). Finally, in Section 7 we draw some conclusions about the possible extensions to our work.

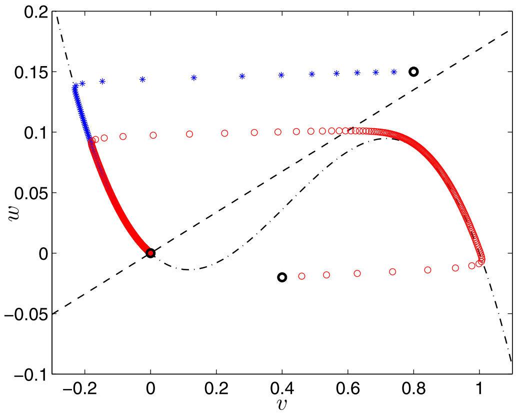


**Fig. 1.** Phase diagram of the FitzHugh–Nagumo local kinetics with $a = 0.16875$, $b = 1$, $\lambda = -100$, $\theta = 0.25$, $d = 1$. Two trajectories starting from the states $(0.4, -0.02)$ and $(0.8, 0.15)$ and reaching the equilibrium $(0, 0)$.

### 1.2. The two-dimensional tridomain model

In this subsection we present a mathematical model for the propagation of electrical excitation in a thin piece of cardiac tissue in contact with an anisotropic volume conductor. We stress that here we dis-consider some 3D effects of the heart by assuming that both the tissue and bath have a small thickness of size $h$ (see [12] for more details). Herein, the bath plane is situated at a distance of $h$ from the tissue domain. The spatial domain for our model is a bounded open subset $\Omega \subset \mathbb{R}^2$ with a piecewise smooth boundary $\partial\Omega$. This represents a two-dimensional slice of the cardiac muscle regarded as two interpenetrating, superimposed and anisotropic continuous media, namely the intracellular ($i$), and extracellular ($e$) tissues. These tissues occupy the same two-dimensional area, and are separated from each other (and connected at each point) by the cardiac cellular membrane. The quantities of interest are *intracellular*, *extracellular* and the bathing medium electric potentials, $u_i, u_e, u_s$ at $(x,t) \in \Omega_T := \Omega \times (0,T)$. The differences $v_1 = v_1(x,t) := u_i - u_e$ and $v_2 = u_e - u_s$ are known as the transmembrane potential and the depth voltage between the tissue and the bath, respectively. The conductivity of the tissue is represented by the tensors $\mathbf{M}_i(x)$ and $\mathbf{M}_e(x)$ given by $\mathbf{M}_j(x) = \sigma_j^t \mathbf{I} + (\sigma_j^l - \sigma_j^t)\mathbf{a}_l(x)\mathbf{a}_l^T(x)$, where $\sigma_j^l = \sigma_j^l(x) \in C^1(\mathbb{R}^2)$ and $\sigma_j^t = \sigma_j^t(x) \in C^1(\mathbb{R}^2)$, $j \in \{e,i\}$, are the coefficients for intra- and extracellular conductivities. The conductivity tensor of the bathing medium $\mathbf{M}_s$ is assumed to be a diagonal matrix. Herein, $\mathbf{a}_l(x)$ is the unit tangent vector at the point $x$. Consequently, $\sigma_j^l$ and $\sigma_j^t$ represent the conductivities of the tissue along and across the fiber direction at point $x$.

The governing equations (bidomain model in a bath, or *tridomain* model) are given by the following coupled reaction–diffusion system (see [3,12]):

$$\begin{aligned}
&\beta c_m \partial_t v_1 - \nabla \cdot \big(\mathbf{M}_i(x)\nabla u_i\big) + \beta I_{\text{ion}}(v_1, w) = I_i,\\
&\beta c_m \partial_t v_1 + \nabla \cdot \big(\mathbf{M}_e(x)\nabla u_e\big) + \beta I_{\text{ion}}(v_1, w) = I_e + g(v_2),\\
&-\nabla \cdot \big(\mathbf{M}_s(x)\nabla u_s\big) = I_s + g(v_2),\\
&\partial_t w - H(v_1, w) = 0, \qquad (x,t) \in \Omega_T.
\end{aligned} \tag{1.1}$$

Here, $c_m > 0$ is the so-called *surface capacitance* of the membrane, $\beta$ is the surface-to-volume ratio, and $w(x,t)$ is the gating or recovery variable, which represents the ionic current variables. The externally applied stimuli to the different media are represented by the functions $I_j(x,t)$, $j = i,e,s$. The functions $H(v_1,w)$ and $I_{\text{ion}}(v_1,w)$ correspond to the widely known FitzHugh–Nagumo model [13,27], based on macroscopic phenomenological evidence and which is often used to avoid computational difficulties arising from a large number of coupling variables. This model is specified by the following reaction terms (adapted to include the description of the field $v_2$)

$$H(v_1,w) = av_1 - bw, \qquad g(v_2) = d^{-1}\Gamma^{-1}v_2, \qquad I_{\text{ion}}(v_1,w) = -\lambda\big(w - v_1(1-v_1)(v_1-\theta)\big),$$

where $\Gamma$ is the "depth" resistance between the bath and depth of the tissue, and $d$ corresponds to the depth, and $a$, $b$, $\lambda$, $\theta$ are given parameters. Fig. 1 presents some details on the local dynamics of the FitzHugh–Nagumo model. The nullclines of the system are the solution curves for

$$v_1 = \phi(w) := \frac{bw}{a}, \qquad w = \varphi(v_1) := v_1(1-v_1)(v_1-\theta),$$

which intersect at the equilibrium point $(0,0)$.

We utilize zero flux boundary conditions, representing an isolated piece of cardiac tissue:

$$\big(\mathbf{M}_j(x)\nabla u_j\big) \cdot \mathbf{n} = 0 \quad \text{on } \Sigma_T := \partial\Omega \times (0,T), \quad j \in \{e,i,s\}, \tag{1.2}$$

and impose the following initial conditions (which are degenerate for the transmembrane potential $v_1$):

$$v_1(0,x) = v_{1,0}(x), \qquad w(0,x) = w_0(x), \quad x \in \Omega. \tag{1.3}$$

An equivalent formulation in the $v_1$, $u_e$, $u_s$, $w$ variables, which is more suitable from the implementation viewpoint, is given by

$$\begin{aligned}
&\beta c_m \partial_t v_1 + \nabla \cdot \big(\mathbf{M}_e(x)\nabla u_e\big) + \beta I_{\mathrm{ion}}(v_1, w) = I_e + g(u_e - u_s),\\
&-\nabla \cdot \big(\mathbf{M}(x)\nabla u_e\big) = \nabla \cdot \big(\mathbf{M}_i(x)\nabla v_1\big) - g(u_e - u_s) + (I_i - I_e),\\
&-\nabla \cdot \big(\mathbf{M}_s(x)\nabla u_s\big) = I_s + g(u_e - u_s),\\
&\partial_t w - H(v_1, w) = 0, \qquad (x,t) \in \Omega_T.
\end{aligned}$$

Herein, $\mathbf{M}(x) = \mathbf{M}_i(x) + \mathbf{M}_e(x)$.

The following compatibility condition is also needed:

$$\int_\Omega u_e(x,t)\,dx = 0 \quad \text{for a.e. } t \in (0,T). \tag{1.4}$$

This condition is only included in order to deal with the well-known degeneracy in time of the bidomain equations. The electric potentials $u_i$ and $u_e$ are determined up to the same additive time-dependent constant, whereas $v_1$ is uniquely determined.

**Remark 1.1.** Note that we should add an additional compatibility condition to (1.4) concerning the relation between the stimuli to the different media:

$$\int_\Omega I_s\,dx = \int_\Omega I_i\,dx - \int_\Omega I_e\,dx = 0. \tag{1.5}$$

Observe that in our model the intra and extracellular domains of the cardiac tissue are spatially mixed, i.e., are on a same spatial plane. However, when the depth resistance is very high ($\Gamma \to +\infty$), system (1.1) boils down to the standard bidomain equations.

## 2. Preliminaries and well-posedness of the state equations

By $H^m(\Omega)$ we denote the usual Sobolev space of order $m$. Since the electrical potentials $u_i$ and $u_e$ are defined up to an additive constant, we use the quotient space $\tilde{H}^1(\Omega) = H^1(\Omega)/\{u \in H^1(\Omega),\ u \equiv \text{Const}\}$. Given $T > 0$ and $1 \leqslant p \leqslant \infty$, $L^p(0,T;\mathbb{R})$ denotes the space of $L^p$ integrable functions from the interval $[0,T]$ into $\mathbb{R}$.

We assume that the functions $\mathbf{M}_j$, $j \in \{e,i,s\}$, $I_{\mathrm{ion}}$, $g$ and $H$ are sufficiently smooth so that the following definitions of weak solutions make sense. Furthermore, we assume that $\mathbf{M}_j \in L^\infty(\Omega)$ and $\mathbf{M}_j\boldsymbol{\xi} \cdot \boldsymbol{\xi} \geqslant C_M|\boldsymbol{\xi}|^2$ for a.e. $x \in \Omega$, for all $\boldsymbol{\xi} \in \mathbb{R}^2$, $j \in \{e,i,s\}$, and a constant $C_M > 0$. For later reference, we now state the definition of a weak solution for the tridomain.

**Definition 2.1.** A sextuple $\mathbf{u} = (v_1, v_2, u_i, u_e, u_s, w)$ of functions is a *weak solution of the tridomain model* (1.1)–(1.3) if $u_s \in L^2(0,T;H^1(\Omega))$, $u_i, u_e \in L^2(0,T;\tilde{H}^1(\Omega))$, $w \in C([0,T], L^2(\Omega))$ with $v_1 = u_i - u_e$ and $v_2 = u_e - u_s$, (1.4) is satisfied, and the following identities hold for all test functions $\varphi_j, \phi \in \mathcal{D}([0,T) \times \bar{\Omega})$, $j = i,e,s$:

$$\begin{aligned}
&\iint_{\Omega_T} \big\{-\beta c_m v_1 \partial_t \varphi_i + \mathbf{M}_i(x)\nabla u_i \cdot \nabla\varphi_i + \beta I_{\mathrm{ion}}\varphi_i\big\}\,dx\,dt - \beta c_m \int_\Omega v_{1,0}(x)\varphi_i(0,x)\,dx = \iint_{\Omega_T} I_i\varphi_i\,dx\,dt,\\
&\iint_{\Omega_T} \big\{-\beta c_m v_1 \partial_t \varphi_e - \mathbf{M}_e(x)\nabla u_e \cdot \nabla\varphi_e + \beta I_{\mathrm{ion}}\varphi\big\}\,dx\,dt \ - \beta c_m \int_\Omega v_{1,0}(x)\varphi_e(0,x)\,dx = \iint_{\Omega_T} \big(I_e + g(v_2)\big)\varphi_e\,dx\,dt,\\
&\iint_{\Omega_T} \mathbf{M}_s(x)\nabla u_s \cdot \nabla\varphi_s = \iint_{\Omega_T} \big(I_s + g(v_2)\big)\varphi_s\,dx\,dt,\\
&-\int_\Omega w_0(x)\phi(0,x)\,dx - \iint_{\Omega_T} w\,\partial_t\phi\,dx\,dt = \iint_{\Omega_T} H(v_1,w)\phi\,dx\,dt.
\end{aligned}$$

**Theorem 2.1** *(Tridomain model). Assume that $v_{1,0} \in L^2(\Omega)$ or $v_{1,0} \in H^1(\Omega)$ and $I_i, I_e, I_s \in L^2(\Omega_T)$. Then the tridomain problem* (1.1)–(1.3) *possesses a unique weak solution.*

**Proof.** (Sketched.) The proof of the existence result is based on introducing the following nondegenerate approximation system:

$$\beta c_m \partial_t v_1 + \varepsilon \partial_t u_i - \nabla \cdot \big(\mathbf{M}_i(x)\nabla u_i\big) + \beta I_{\mathrm{ion}}(v_1, w) = I_i,$$
$$\beta c_m \partial_t v_1 - \varepsilon \partial_t u_e + \nabla \cdot \big(\mathbf{M}_e(x)\nabla u_e\big) + \beta I_{\mathrm{ion}}(v_1, w) = I_e + g(v_2),$$
$$-\nabla \cdot \big(\mathbf{M}_s(x)\nabla u_s\big) = I_s + g(v_2),$$
$$\partial_t w - H(v_1, w) = 0, \qquad (x,t) \in \Omega_T,$$

where $\varepsilon > 0$ is a small number.

*The case* $v_0 = u_{i,0} - u_{e,0}$ *with* $u_{i,0}, u_{e,0} \in H^1(\Omega)$. The result in [5], provide us with the existence of the sequences of functions $(u_{i,\varepsilon})_{\varepsilon>0}$, $(u_{e,\varepsilon})_{\varepsilon>0}$, $(u_{s,\varepsilon})_{\varepsilon>0}$, $(w_\varepsilon)_{\varepsilon>0}$, $(v_{1,\varepsilon} = u_{i,\varepsilon} - u_{e,\varepsilon})_{\varepsilon>0}$ and $(v_{2,\varepsilon} = u_{e,\varepsilon} - u_{s,\varepsilon})_{\varepsilon>0}$: $u_{s,\varepsilon} \in L^2(0,T;H^1(\Omega))$, $u_{i,\varepsilon}, u_{e,\varepsilon} \in L^2(0,T;\tilde{H}^1(\Omega))$, $w_\varepsilon \in C(0,T;L^2(\Omega))$, such that $\partial_t u_{j,\varepsilon}, \partial_t w_\varepsilon \in L^2(\Omega_T)$, $u_j(0) = u_{j,0}$ a.e. in $\Omega$, for $j = i, e$, and satisfying the weak formulation

$$\iint_{\Omega_T} \beta c_m \partial_t v_{1,\varepsilon} \varphi_i \,dx\,dt + \iint_{\Omega_T} \varepsilon \partial_t u_{i,\varepsilon} \varphi_i \,dx\,dt + \iint_{\Omega_T} \mathbf{M}_i(x)\nabla u_{i,\varepsilon} \cdot \nabla \varphi_i \,dx\,dt + \beta \iint_{\Omega_T} I_{\mathrm{ion}}(v_{1,\varepsilon}, w_\varepsilon)\varphi_i \,dx\,dt$$
$$= \iint_{\Omega_T} I_{i,\varepsilon} \varphi_i \,dx\,dt, \tag{2.1}$$

$$\iint_{\Omega_T} \beta c_m \partial_t v_{1,\varepsilon} \varphi_e \,dx\,dt - \iint_{\Omega_T} \varepsilon \partial_t u_{e,\varepsilon} \varphi_e \,dx\,dt - \iint_{\Omega_T} \mathbf{M}_e(x)\nabla u_{e,\varepsilon} \cdot \nabla \varphi_e \,dx\,dt + \beta \iint_{\Omega_T} I_{\mathrm{ion}}(v_{1,\varepsilon}, w_\varepsilon)\varphi_e \,dx\,dt$$
$$= \iint_{\Omega_T} \big(I_{e,\varepsilon} + g(v_{2,\varepsilon})\big)\varphi_e \,dx\,dt, \tag{2.2}$$

$$\iint_{\Omega_T} \mathbf{M}_s(x)\nabla u_{s,\varepsilon} \cdot \nabla \varphi_s = \iint_{\Omega_T} \big(I_{s,\varepsilon} + g(v_{2,\varepsilon})\big)\varphi_s \,dx\,dt, \tag{2.3}$$

$$\iint_{\Omega_T} \partial_t w_\varepsilon \phi \,dx\,dt = \iint_{\Omega_T} H(v_{1,\varepsilon}, w_\varepsilon)\phi \,dx\,dt, \tag{2.4}$$

for all $\varphi_j \in L^2(0,T;\tilde{H}^1(\Omega))$, $\varphi_s \in L^2(0,T;H^1(\Omega))$ and $\phi \in C(0,T;L^2(\Omega))$, $j = i, e$.

Substituting $\varphi_i = u_{i,\varepsilon}$, $\varphi_e = -u_{e,\varepsilon}$, $\varphi_s = u_{s,\varepsilon}$ and $\phi = w_\varepsilon$ in (2.1), (2.2), (2.3) and (2.4), respectively, and then summing the resulting equations, we have immediately at our disposal the following series of a priori estimates: there exists a constant $C > 0$ not depending on $\varepsilon$ such that

$$\|v_{1,\varepsilon}\|_{L^\infty(0,T;L^2(\Omega))} + \sum_{j=i,e,} \|\sqrt{\varepsilon} u_{j,\varepsilon}\|_{L^\infty(0,T;L^2(\Omega))} + \|\nabla u_{j,\varepsilon}\|_{L^2(\Omega_T)} \leqslant C,$$
$$\|\nabla u_{s,\varepsilon}\|_{L^2(\Omega_T)} + \|u_{s,\varepsilon}\|_{L^2(\Omega_T)} + \leqslant C, \qquad \|\partial_t w_\varepsilon\|_{C(0,T;L^2(\Omega))} \leqslant C. \tag{2.5}$$

In addition

$$\|\partial_t v_{1,\varepsilon}\|_{L^2(\Omega_T)} + \sum_{j=i,e} \|\sqrt{\varepsilon}\partial_t u_{j,\varepsilon}\|_{L^2(\Omega_T)} \leqslant C. \tag{2.6}$$

Exploiting (2.5) and (2.6), we can assume there exist limit functions $u_i$, $u_e$, $u_s$, $w$, $v_1$, $v_2$ with $v_1 = u_i - u_e$ and $v_2 = u_e - u_s$ such that as $\varepsilon \to 0$ the following convergences hold (modulo extraction of subsequences, which for simplicity we do not relabel):

$$\begin{cases} v_{1,\varepsilon} \to v_1 \quad \text{a.e. in } \Omega_T, \text{ strongly in } L^2(\Omega_T), \text{ and weakly in } L^2\big(0,T;\tilde{H}^1(\Omega)\big), \\ u_{s,\varepsilon} \to u_s \quad \text{a.e. in } \Omega_T, \text{ strongly in } L^2(\Omega_T), \text{ and weakly in } L^2\big(0,T;H^1(\Omega)\big), \\ u_{j,\varepsilon} \to u_j \quad \text{weakly in } L^2\big(0,T;\tilde{H}^1(\Omega)\big) \text{ for } j = i, e, \\ I_{\mathrm{ion}}(v_{1,\varepsilon}, w_\varepsilon) \to I_{\mathrm{ion}}(v_1, w), \quad g(v_{2,\varepsilon}) \to g(v_2), \quad \text{and} \\ H(v_{1,\varepsilon}, w_\varepsilon) \to H(v_1, w) \quad \text{a.e. in } \Omega_T \text{ and weakly in } L^2(\Omega_T), \end{cases} \tag{2.7}$$

and, according to (2.6), $v \in C([0,T];L^2(\Omega))$. Additionally, $\partial_t v_{1,\varepsilon} \to \partial_t v_1$ and $\varepsilon \partial_t u_{j,\varepsilon} \to 0$, $j = i, e$, weakly in $L^2(\Omega_T)$. Arguing as in [5], we conclude also that $I_{\mathrm{ion}}(v_{1,\varepsilon}, w_\varepsilon) \to I_{\mathrm{ion}}(v_1, w)$, $g(v_{2,\varepsilon}) \to g(v_2)$ and $H(v_{1,\varepsilon}, w_\varepsilon) \to H(v_1, w)$ strongly in

$L^2(\Omega_T)$. Thanks to the convergences (2.7), we readily see that the limit $(u_i, u_e, u_s, w, v_1 = u_i - u_e, v_2 = u_e - u_s)$ is a weak solution of the tridomain model (1.1), (1.2), (1.3) when $v_0 \in H^1(\Omega)$.

*The case* $v_{1,0} \in L^2(\Omega)$. To deal with this case, we approximate the initial data $v_0$ by a sequence $(v_{1,0,\rho})_{\rho>0}$ of functions satisfying

$$v_{1,0,\rho} \in C_0^\infty(\Omega), \quad \|v_{1,0,\rho}\|_{L^2(\Omega)} \leqslant \|v_{1,0}\|_{L^2(\Omega)}, \qquad v_{1,0,\rho} \to v_{1,0} \quad \text{in } L^2(\Omega) \quad \text{as } \rho \to 0.$$

This fact will imply the existence of sequences $(u_{i,\rho})_{\rho>0}$, $(u_{e,\rho})_{\rho>0}$, $(u_{s,\rho})_{\rho>0}$, $(w_\rho)_{\rho>0}$, $(v_{1,\rho} = u_{i,\rho} - u_{e,\rho})_{\rho>0}$ and $(v_{2,\rho} = u_{e,\rho} - u_{s,\rho})_{\rho>0}$ for which $u_{i,\rho}, u_{e,\rho} \in L^2(0,T;\tilde{H}^1(\Omega))$, $u_{s,\rho} \in L^2(0,T;H^1(\Omega))$, $w_\rho \in C(0,T;L^2(\Omega))$, and

$$\iint_{\Omega_T} \beta c_m \partial_t v_{1,\rho}\varphi_i \,dx\,dt + \iint_{\Omega_T} \mathbf{M}_i(x)\nabla u_{i,\rho}\cdot\nabla\varphi_i \,dx\,dt + \beta\iint_{\Omega_T} I_{\text{ion}}(v_{1,\rho}, w_\rho)\varphi_i \,dx\,dt = \iint_{\Omega_T} I_i\varphi_i \,dx\,dt, \tag{2.8}$$

$$\iint_{\Omega_T} \beta c_m \partial_t v_{1,\rho}\varphi_e \,dx\,dt - \iint_{\Omega_T} \mathbf{M}_e(x)\nabla u_{e,\rho}\cdot\nabla\varphi_e \,dx\,dt + \beta\iint_{\Omega_T} I_{\text{ion}}(v_{1,\rho}, w_\rho)\varphi_e \,dx\,dt = \iint_{\Omega_T} \big(I_e + g(v_{2,\rho})\big)\varphi_e \,dx\,dt, \tag{2.9}$$

$$\iint_{\Omega_T} \mathbf{M}_s(x)\nabla u_{s,\rho}\cdot\nabla\varphi_s = \iint_{\Omega_T} \big(I_s + g(v_{2,\rho})\big)\varphi_s \,dx\,dt, \tag{2.10}$$

$$\iint_{\Omega_T} \partial_t w_\rho \phi \,dx\,dt = \iint_{\Omega_T} H(v_{1,\rho}, w_\rho)\phi \,dx\,dt, \tag{2.11}$$

for all $\varphi_j \in L^2(0,T;\tilde{H}^1(\Omega))$, $\varphi_s \in L^2(0,T;H^1(\Omega))$, $\phi \in C(0,T;L^2(\Omega))$, $j = i, e$.

To pass to the limit $\rho \to 0$ in (2.8), (2.9), (2.10) and (2.11) we need a priori estimates. The ones from the first case that are still $\rho$-independent are

$$\|v_{1,\rho}\|_{L^\infty(0,T;L^2(\Omega))} + \|w_\rho\|_{L^\infty(0,T;L^2(\Omega))} \leqslant c, \qquad \|\nabla u_{j,\rho}\|_{L^2(\Omega_T)} \leqslant c,$$
$$\|u_{j,\rho}\|_{L^2(\Omega_T)} + \|w_\rho\|_{C(0,T;L^2(\Omega))} \leqslant c, \quad j = i, e, s.$$

Therefore the sequences $(u_{j,\rho})_{\rho>0}$ and $(u_{s,\rho})_{\rho>0}$, are bounded in $L^2(0,T;\tilde{H}^1(\Omega))$ and $L^2(0,T;H^1(\Omega))$, respectively for $j = i, e$ with $v_{1,\rho} = u_{i,\rho} - u_{e,\rho}$ and $v_{2,\rho} = u_{e,\rho} - u_{s,\rho}$. In view of the equations satisfied by $v_{1,\rho}$ this implies that $(\partial_t v_{1,\rho})_{\rho>0}$ is bounded in $L^2(0,T;(\tilde{H}^1(\Omega))')$. Therefore, possibly at the cost of extracting subsequences (which are not relabeled), we can assume that there exist limits $u_i, u_e \in L^2(0,T;\tilde{H}^1(\Omega))$ and $u_s \in L^2(0,T;H^1(\Omega))$ with $v_1 = u_i - u_e$ and $v_2 = u_e - u_s$ such that as $\rho \to 0$

$$\begin{cases} v_{1,\rho} \to v_1 \quad \text{a.e. in } \Omega_T, \text{ strongly in } L^2(\Omega_T), \text{ and weakly in } L^2\big(0,T;\tilde{H}^1(\Omega)\big), \\ u_{s,\rho} \to u_s \quad \text{a.e. in } \Omega_T, \text{ strongly in } L^2(\Omega_T), \text{ and weakly in } L^2\big(0,T;H^1(\Omega)\big), \\ u_{j,\rho} \to u_j \quad \text{weakly in } L^2\big(0,T;\tilde{H}^1(\Omega)\big) \text{ for } j = i, e, s, \\ w_\rho \to w \quad \text{weakly in } L^2(\Omega_T), \\ I_{\text{ion}}(v_{1,\rho}, w_\rho) \to I_{\text{ion}}(v_1, w), \quad g(v_{2,\rho}) \to g(v_2), \quad \text{and} \\ H(v_{1,\rho}, w_\rho) \to H(v_1, w) \quad \text{a.e. in } \Omega_T \text{ and weakly in } L^2(\Omega_T), \end{cases} \tag{2.12}$$

and $v_1 \in C([0,T];L^2(\Omega))$. Arguing as in the proof of the first case, we obtain that $I_{\text{ion}}(v_{1,\varepsilon}, w_\varepsilon) \to I_{\text{ion}}(v_1, w)$, $g(v_{2,\varepsilon}) \to g(v_2)$, and $H(v_{1,\rho}, w_\rho) \to H(v_1, w)$ strongly in $L^2(\Omega_T)$. Equipped with these convergences it is not difficult to pass to the limit as $\rho \to 0$ in (2.8)–(2.11) to conclude that the limit $(u_i, u_e, u_s, w, v_1 = u_i - u_e, v_2 = u_e - u_s)$ is a weak solution to the tridomain model (1.1), (1.2), (1.3).

Finally, applying the same techniques used in [5], we deduce the uniqueness of the weak solution $(u_i, u_e, u_s, w, v_1, v_2)$. This proves Theorem 2.1. $\square$

## 3. The optimal control problem

In this section we present the optimal control problem governed by the tridomain model, and we prove existence of an optimal control using the arguments of e.g. [24,34]. We stress that the major part of the analysis in this section is formal.

A cost functional which is suitable to optimize the transmembrane potential and bath current is given by

$$J(I_s) = \frac{1}{2}\left(\int_0^T \left(\int_{\Omega_o} |v_1|^2\, dx + \alpha \int_{\Omega_c} |I_s|^2\, dx\right) dt\right).$$

Here $\Omega_o$ and $\Omega_c$ denote the observation and control sub-domains, and $\alpha > 0$ denotes a regularization parameter. The objective is to damp the transmembrane potential $v_1$ in $\Omega_o$.

We seek to reconstruct an unknown function $I_s$ by solving the minimization problem

$$\min_{I_s} J(I_s) \quad \text{subject to (1.1), (1.5)}. \tag{3.1}$$

Notice that here Eqs. (1.1) play the role of constraints for the solution. The following lemma states the existence of an optimal solution for (3.1).

**Lemma 3.1.** *Given $v_{1,0} \in L^2(\Omega)$ and the control $I_s \in L^2(\Omega_T)$, there exists a solution $(v_1^*, I_s^*)$ of the optimal control problem* (3.1).

**Proof.** Note that since $J$ is bounded, there exists a minimizing sequence $(I_{s,n})_n$ of (3.1) such that $J(I_{s,n})$ converges to the infimum of $J(I_s)$ over all feasible $I_s$ (recall that for each $I_{s,n}$ corresponds to a solution $(u_{i,n}, u_{e,n}, u_{s,n}, v_{1,n}, v_{2,n}, w_n)$ of (1.1), (1.2), (1.3)). Herein, we have used the compactness of $(v_{1,n})_n$ in $L^2(Q_T)$ and the lower-semicontinuity of the second integral in $J$ with respect to the weak $L^2$ topology. Next we use (2.12) (where $\rho$ and $(u_i, u_e, u_s, v_1, v_2, w)$ are replaced by $n$ and $(u_i^*, u_e^*, u_s^*, v_1^*, v_2^*, w^*)$), the weak convergence of $I_{n,s}$ to $I_s^*$ in $L^2(\Omega_T)$ to conclude that $I_s^*$ satisfies (1.5) and (1.1), (1.2), (1.3) in weak sense. □

Next we introduce the Lagrange functional $\mathcal{L}$ related to the optimal control problem (3.1) for the primal variables $(u_i, u_e, u_s, w)$ (or equivalently $(v_1, u_e, u_s, w)$) and the dual variables $(p_i, p_e, p_s, q)$ (equivalently $(p_1, p_e, p_s, q)$)

$$\begin{aligned}
\mathcal{L}(u_i, u_e, u_s, I_s, p_i, p_e, p_s, w, q) &= \frac{1}{2}\left(\int_0^T\int_{\Omega_o} |v_1|^2\, dx\, dt + \alpha \int_0^T\int_{\Omega_c} |I_s|^2\, dx\, dt\right) \\
&\quad + \int_0^T\int_{\Omega_o} \big(\beta c_m \partial_t v_1 - \nabla\cdot\big(\mathbf{M}_i(x)\nabla u_i\big) + \beta I_{\text{ion}}(v_1, w) - I_i\big) p_i\, dx\, dt \\
&\quad - \int_0^T\int_{\Omega_o} \big(\beta c_m \partial_t v_1 + \nabla\cdot\big(\mathbf{M}_e(x)\nabla u_e\big) + \beta I_{\text{ion}}(v_1, w) - g(v_2) - I_e\big) p_e\, dx\, dt \\
&\quad - \int_0^T\int_{\Omega_o} \big(\nabla\cdot\big(\mathbf{M}_s(x)\nabla u_s\big) + g(v_2) + I_s\big) p_s\, dx\, dt \\
&\quad + \int_0^T\int_{\Omega_o} \big(\partial_t w - H(v_1, w)\big) q\, dx\, dt.
\end{aligned} \tag{3.2}$$

From (3.2) we get

$$\left(\frac{\partial \mathcal{L}(u_i, u_e, u_s, I_s, p_i, p_e, p_s, w, q)}{\partial I_s}, \delta I_s\right) = (\alpha I_s - p_s, \delta I_s),$$

that is, $\nabla_{I_s}\mathcal{L}(u_i, u_e, u_s, I_s, p_i, p_e, p_s, w, q) = \alpha I_s - p_s$, and therefore the optimality is given if

$$I_s = \frac{p_s}{\alpha}.$$

The first order optimality system characterizing the adjoint variables, is given by the Lagrange multipliers which result from equating the partial derivatives of $\mathcal{L}$ with respect to $u_i$, $u_e$, $u_s$ and $w$ equal to zero

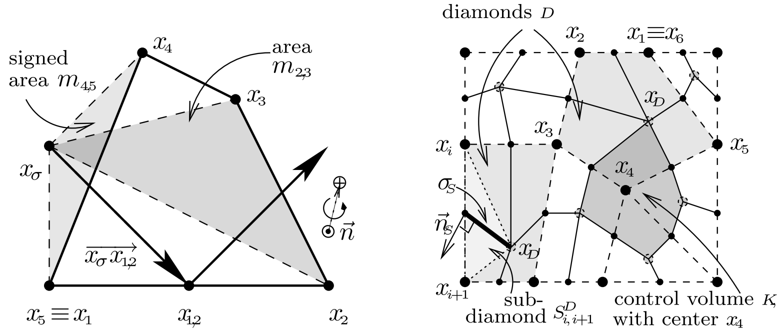


**Fig. 2.** Sketch of the diamond mesh $\mathfrak{D}$ and the corresponding dual mesh $\overline{\mathfrak{M}}$.

$$-\beta c_m \partial_t(p_i - p_e) - \nabla\cdot\big(\mathbf{M}_i(x)\nabla p_i\big) + \beta I_{\mathrm{ion}u_i}(v_1, w)(p_i - p_e) - H_{u_i}(v_1, w)q + v_1 = 0,$$
$$\beta c_m \partial_t(p_i - p_e) - \nabla\cdot\big(\mathbf{M}_e(x)\nabla p_e\big) - \beta I_{\mathrm{ion}u_e}(v_1, w)(p_i - p_e) + H_{u_e}(v_1, w)q - v_1 = -g_{u_e}(v_2)(p_e - p_s),$$
$$-\nabla\cdot\big(\mathbf{M}_s(x)\nabla p_s\big) = g_{u_s}(v_2)(p_e - p_s) - \partial_t q + \beta I_{\mathrm{ion}w}(v_1, w)(p_i - p_e) - H_w(v_1, w)q = 0, \qquad (x,t) \in \Omega_T. \tag{3.3}$$

Herein $I_{\mathrm{ion}u_i}$, $I_{\mathrm{ion}u_e}$, $g_{u_e}$, $g_{u_s}$, and $H_w$ are the derivatives of $I_{\mathrm{ion}}$ and $H$ with respect to $v_1$, $u_e$, $u_s$, and $w$, respectively. We complete system (3.3) with terminal conditions and boundary conditions:

$$p_i(T), p_e(T) = 0 \quad \text{and} \quad q(T) = 0,$$
$$\mathbf{M}_i(x)\nabla p_j \cdot \eta = 0 \quad \text{on } \Sigma_T \quad \text{for } j = i, e, s, \tag{3.4}$$

and a condition analogous to (1.4), required for $p_e$:

$$\int_\Omega p_e \, dx = 0.$$

From the analysis above, the gradient of the reduced cost functional is written as

$$\nabla \hat{J}(I_s) = \alpha I_s - p_s.$$

For the evaluation of this gradient, we first need to solve the state system (1.1) and then the coupled adjoint system (3.3).

## 4. Finite volume approximation

In this section we construct a finite volume scheme for the direct problem with anisotropic conductivities $\mathbf{M}_j$ for $j = i, e, s$. We prove existence of discrete solutions to this scheme, and we show that it converges to a weak solution. To define the FV scheme for approximating solutions to the tridomain equations (1.1)–(1.3), we follow the framework developed in [1].

Let $\Omega \subset \mathbb{R}^2$ be a bounded polygonal domain. A *partition* of $\Omega$ is a finite set of disjoint open polygons such that $\Omega$ is their union, up to a set of measure zero. The mesh we consider is actually the couple $(\mathfrak{D}, \overline{\mathfrak{M}})$, which we denote by $\mathfrak{T}$. We take $\mathfrak{D}$ a partition of $\Omega$; each element of $\mathfrak{D}$ is denoted by $D$ and called a *diamond cell*. Each $D \in \mathfrak{D}$ is supplied with a center $x_D$; for the sake of simplicity, one may assume that $x_D \in D$ and $D$ is convex. In practice, $\mathfrak{D}$ can be a triangulation of $\Omega$. For each $D \in \mathfrak{D}$, we fix a counter-clockwise numbering of its vertices by $x_1, \ldots, x_l$ ($l \geqslant 3$), letting $l + 1 := 1$.

We set $x_{i,i+1} = 0.5(x_i + x_{i+1})$ (the middle-point of the segment $[x_i, x_{i+1}]$). A generic vertex of $\mathfrak{D}$ is denoted by $x_K$. Each $x_K$ is the center of a *control volume* $K$, as shown in Fig. 2. The mesh $\overline{\mathfrak{M}} = \mathfrak{M} \cup \partial\mathfrak{M}$ is the *median dual mesh* of $\mathfrak{D}$ (see [16]). In the case $x_K \in \partial\Omega$, we write $K \in \partial\mathfrak{M}$; if $x_K \in \Omega$, we write $K \in \mathfrak{M}$. In the case each $D$ is an inscribed polygon and $x_D$ is the center of its circumscribed circle, the median dual mesh $\overline{\mathfrak{M}}$ coincides with the Voronoï dual mesh of $\mathfrak{D}$. Each diamond $D \in \mathfrak{D}$ is a polygon with vertices $x_1 = x_{K_1}, \ldots, x_l = x_{K_l}$; it is split into $l$ *sub-diamonds* $S^D_{i,i+1}$ which are the triangles with vertices $x_D$, $x_i$, $x_{i+1}$. For $K \in \mathfrak{M}$, $\mathcal{V}(K)$ is the set of all sub-diamonds having $x_K$ for a vertex. The set of all sub-diamonds is denoted by $\mathfrak{S}$. In a sub-diamond $S = S^D_{i,i+1}$, we denote by $\sigma_S$ the part of $\partial K_i \cap \partial K_{i+1}$ included into $S$; we denote its length by $m_S$. We have $\sigma_S \equiv [x_D, x_{i,i+1}]$; denote by $\vec{n}_S$ its unit normal vector such that $\vec{n}_S = \vec{n} \times \overrightarrow{x_D x_{i,i+1}}/m_S$ (if $m_S \equiv \|\overrightarrow{x_D x_{i,i+1}}\| = 0$, $\vec{n}_S$ is arbitrary). Finally, for $K \in \mathfrak{M}$ and $S \in \mathcal{V}(K)$, set $\epsilon^K_S := 0$ if $K = K_i$, and $\epsilon^K_S := 1$ if $K = K_{i+1}$.

**Remark 4.1.** Diamonds (respectively, sub-diamonds) serve to define the gradient (respectively, divergence) operator between the spaces of discrete functions and discrete fields defined below.

A *discrete function on $\Omega$* is a set $w^{\mathfrak{T}} = (w_K)_{K\in\mathfrak{M}}$ of real values. The set of all such functions is denoted by $\mathbb{R}^{\mathfrak{T}}$. Whenever convenient, a discrete function $w^{\mathfrak{T}}$ is identified with the function

$$x \in \Omega \mapsto \sum_{K\in\mathfrak{M}} w_K \mathbb{1}_K(x).$$

Similarly, a *discrete function on $\overline{\Omega}$* is a set $w^{\overline{\mathfrak{T}}} = (w_K)_{K\in\overline{\mathfrak{M}}}$. The set of all such functions is denoted by $\mathbb{R}^{\overline{\mathfrak{T}}}$. On $\mathbb{R}^{\mathfrak{T}}$, we define the scalar product:

$$[\![ w^{\mathfrak{T}}, v^{\mathfrak{T}} ]\!] = \sum_{K\in\mathfrak{M}} Vol(K) w_K v_K,$$

where $Vol(S)$ is the measure of $S \subset \mathbb{R}^2$. A *discrete* (respectively, scalar) *field on $\Omega$* is a set $\vec{\mathcal{M}}^{\mathfrak{T}} = (\vec{\mathcal{M}}_D)_{D\in\mathfrak{D}}$ in $\mathbb{R}^2$ (respectively, in $\mathbb{R}$). If a sub-diamond $S$ is included into $D$, we set $\vec{\mathcal{M}}_S := \vec{\mathcal{M}}_D$. The set of all discrete fields is denoted by $(\mathbb{R}^2)^{\mathfrak{D}}$. We identify $\vec{\mathcal{M}}^{\mathfrak{T}}$ with the function $x \in \Omega \mapsto \sum_{D\in\mathfrak{D}} \vec{\mathcal{M}}_D \mathbb{1}_D(x)$, and define on $(\mathbb{R}^2)^{\mathfrak{D}}$ the scalar product:

$$\{\!\{ \vec{\mathcal{M}}^{\mathfrak{T}}, \vec{\mathcal{G}}^{\mathfrak{T}} \}\!\} = \sum_{D\in\mathfrak{D}} Vol(D) \vec{\mathcal{M}}_D \cdot \vec{\mathcal{G}}_D.$$

We define the *discrete gradient* operator $\nabla^{\mathfrak{T}} : w^{\overline{\mathfrak{T}}} \in \mathbb{R}^{\overline{\mathfrak{T}}} \mapsto (\nabla_D w^{\overline{\mathfrak{T}}})_{D\in\mathfrak{D}} \in (\mathbb{R}^2)^{\mathfrak{D}}$. The value $\nabla_D w^{\overline{\mathfrak{T}}}$ is reconstructed in [1] from the values $w_1 = w_{K_1}, \ldots, w_l = w_{K_l}$ of $w^{\overline{\mathfrak{T}}}$ at the vertices $x_1 = x_{K_1}, \ldots, x_l = x_{K_l}$ of $D$.

Consider the simplest case where we take $\mathfrak{M}$ as a partition into triangles. In this case, the vector $\vec{g} =: \nabla_D u^{\mathfrak{T}}$ is assembled from its projection $\vec{p} := \mathrm{Proj}_D \vec{g}$ on the direction $\overrightarrow{x_K x_L}$ ($\mathrm{Proj}_D \vec{g}$ is obtained by two-point interpolation on a line of the values $u_K$, $u_L$ at the points $x_K$, $x_L$)

$$\mathrm{Proj}_D \vec{g} = \frac{u_L - u_K}{|\overrightarrow{x_K x_L}|} \overrightarrow{x_K x_L}.$$

Then we define the *discrete divergence* operator $\mathrm{div}^{\mathfrak{T}} : \vec{\mathcal{M}}^{\mathfrak{T}} \in (\mathbb{R}^2)^{\mathfrak{D}} \mapsto v^{\mathfrak{T}} \in \mathbb{R}^{\mathfrak{T}}$, where $v^{\mathfrak{T}} = (v_K)_{K\in\mathfrak{M}}$ is the discrete function on $\Omega$ with the entries $v_K$ given by

$$\mathrm{div}^{\mathfrak{T}} \mathcal{M}^{\mathfrak{T}} = \frac{1}{Vol(K)} \sum_{S\in\mathcal{V}(K)} m_S \vec{\mathcal{M}}_S \cdot (-1)^{\epsilon_S^K} \vec{n}_S \equiv \frac{1}{Vol(K)} \sum_{S\in\mathcal{V}(K)} (-1)^{\epsilon_S^K} \langle \vec{\mathcal{M}}_S, \vec{n}, \overrightarrow{x_D x_{i,i+1}} \rangle.$$

Here we mean that each $S$ in $\mathcal{V}(K)$ is of the form $S_{i,i+1}^D$; the notation $\epsilon_S^K$, $x_D$, $x_{i,i+1}$ under the sign "$\sum$" refers to $S_{i,i+1}^D$. The value $Vol(K) v_K$ is the flux of the vector field $\vec{\mathcal{M}}^{\mathfrak{T}}$ through the boundary $\partial K$, thus it represents $\int_K \mathrm{div}\, \vec{\mathcal{M}}^{\mathfrak{T}}$. Indeed, thanks to the constraint $x_D \in D$, whenever $x_K$ is a vertex of $S \subset D$, the vector $(-1)^{\epsilon_S^K} \vec{n}_S$ is the unit normal vector to $\sigma_S \subset \partial K$ exterior to $K$.

**Remark 4.2.** Note that the discrete divergence and gradient operators $\mathrm{div}^{\mathfrak{T}}$, $\nabla^{\mathfrak{T}}$ are linked by the following duality property:

$$\forall w^{\overline{\mathfrak{T}}} \in \mathbb{R}^{\overline{\mathfrak{T}}}\ \forall \vec{\mathcal{M}}^{\mathfrak{T}} \in \left(\mathbb{R}^d\right)^{\mathfrak{D}} \quad [\![ -\mathrm{div}^{\mathfrak{T}}[\vec{\mathcal{M}}^{\mathfrak{T}}], w^{\mathfrak{T}} ]\!] = \{\!\{ \vec{\mathcal{M}}^{\mathfrak{T}}, \nabla^{\mathfrak{T}} w^{\overline{\mathfrak{T}}} \}\!\},$$

where the Neumann boundary condition is taken into account.

Now, we define discrete functions $w^{\mathfrak{T},\Delta t} \in (\mathbb{R}^{\mathfrak{T}})^{N_{\Delta t}}$ on $(0,T) \times \Omega$ as collections of discrete functions $w^{\mathfrak{T},n+1}$ on $\Omega$ parametrized by $n \in [0, N_\Delta t] \cap \mathbb{N}$. Discrete functions $w^{\mathfrak{T},\Delta t} \in (\mathbb{R}^{\mathfrak{T}})^{N_{\Delta t}}$ on $(0,T) \times \overline{\Omega}$ and discrete fields $\vec{\mathcal{M}}^{\mathfrak{T},\Delta t} \in (\mathbb{R}^{\mathfrak{D}})^{N_{\Delta t}}$ are defined similarly.

We define the size of the mesh by

$$\mathrm{size}(\mathfrak{T}) := \max\left\{ \max_{K\in\overline{\mathfrak{M}}} \mathrm{diam}(K), \max_{D\in\mathfrak{D}} \mathrm{diam}(D) \right\}.$$

We define cell averages of the reaction terms:

$$H^{\mathfrak{T},n+1} := H\left(v_1^{\mathfrak{T},n+1}, w^{\mathfrak{T},n+1}\right),$$
$$I_{\mathrm{ion}}^{\mathfrak{T},n+1} := I_{\mathrm{ion}}\left(v_1^{\mathfrak{T},n+1}, w^{\mathfrak{T},n+1}\right),$$

and

$$G^{\mathfrak{T},n+1} := g\left(v_2^{\mathfrak{T},n+1}\right),$$
$$I_{j,K}^{n+1} := \frac{1}{\Delta t|K|} \int_{t^n}^{t^{n+1}} \int_K I_j(x,t)\, dx\, dt, \quad j \in \{i,e,s\}.$$

The computation starts from the initial cell averages

$$v_1^{0,K} = \frac{1}{|K|}\int_K v_{1,0}(x)\,dx, \qquad w_K^0 = \frac{1}{|K|}\int_K w_0(x)\,dx.$$

The finite volume schemes for problem (1.1), (1.2), (1.3) can be formally written under the following general form: find $((u_i^{\mathfrak{T},n}, u_e^{\mathfrak{T},n}, u_s^{\mathfrak{T},n}, v_1^{\mathfrak{T},n}, v_2^{\mathfrak{T},n}, w^{\mathfrak{T},n}))_{n=1,\dots,N} \subset (R^{\mathfrak{T}})^6$ satisfying

$$\begin{aligned}
&\beta c_m \frac{v_1^{\mathfrak{T},n+1} - v_1^{\mathfrak{T},n}}{\Delta t} - \operatorname{div}^{\mathfrak{T}}\big[\mathbf{M}_i^{\mathfrak{T}} \nabla^{\mathfrak{T}} u_i^{\mathfrak{T},n+1}\big] + \beta I_{\text{ion}}^{\mathfrak{T},n+1} = I_i^{\mathfrak{T},n+1},\\
&\beta c_m \frac{v_1^{\mathfrak{T},n+1} - v_1^{\mathfrak{T},n}}{\Delta t} + \operatorname{div}^{\mathfrak{T}}\big[\mathbf{M}_e^{\mathfrak{T}} \nabla^{\mathfrak{T}} u_e^{\mathfrak{T},n+1}\big] + \beta I_{\text{ion}}^{\mathfrak{T},n+1} = I_e^{\mathfrak{T},n+1} + G^{\mathfrak{T},n+1},\\
&-\operatorname{div}^{\mathfrak{T}}\big[\mathbf{M}_i^{\mathfrak{T}} \nabla^{\mathfrak{T}} u_i^{\mathfrak{T},n+1}\big] = I_s^{\mathfrak{T},n+1} + G^{\mathfrak{T},n+1},\\
&\frac{w^{\mathfrak{T},n+1} - w^{\mathfrak{T},n}}{\Delta t} - H^{\mathfrak{T},n+1} = 0,\\
&v_1^{\mathfrak{T},n+1} = \big(u_i^{\mathfrak{T},n+1} - u_e^{\mathfrak{T},n+1}\big),\\
&v_2^{\mathfrak{T},n+1} = \big(u_e^{\mathfrak{T},n+1} - u_s^{\mathfrak{T},n+1}\big).
\end{aligned} \tag{4.1}$$

The compatibility condition (1.4) is discretized via

$$\sum_{K\in\overline{\mathfrak{M}}} Vol(K) u_{e,K} = 0. \tag{4.2}$$

Herein, the matrices $\mathbf{M}_{i,e}^{\mathfrak{T}}(\cdot)$ are the projections of $\mathbf{M}_{i,e}(\cdot)$ on the diamond mesh.

Equivalently, $(u_i^{\mathfrak{T},\Delta t}, u_e^{\mathfrak{T},\Delta t}, u_s^{\mathfrak{T},\Delta t}, v_1^{\mathfrak{T},\Delta t}, v_2^{\mathfrak{T},\Delta t}, w^{\mathfrak{T},\Delta t})$ is a discrete solution if $v_1^{\mathfrak{T},\Delta t} = u_i^{\mathfrak{T},\Delta t} - u_e^{\mathfrak{T},\Delta t}$, $v_2^{\mathfrak{T},\Delta t} = u_e^{\mathfrak{T},\Delta t} - u_s^{\mathfrak{T},\Delta t}$ and for all $\varphi_i^{\mathfrak{T}}, \varphi_e^{\mathfrak{T}}, \varphi_s^{\mathfrak{T}}, \varphi^{\mathfrak{T}} \in R^{\mathfrak{T}}$, for all $n \in [0, N]$ the following identities hold:

$$\begin{cases}
\beta c_m \dfrac{1}{\Delta t} \big[\!\big[ v_1^{\mathfrak{T},n+1} - v_1^{\mathfrak{T},n}, \varphi_i^{\mathfrak{T}} \big]\!\big]_\Omega + \big\{\!\!\big\{ \mathbf{M}_i^{\mathfrak{T}} \nabla^{\mathfrak{T}} u_i^{\mathfrak{T},n+1}, \nabla^{\mathfrak{T}} \varphi_i^{\mathfrak{T}} \big\}\!\!\big\}_\Omega + \big]\!\big] \beta I_{\text{ion}}^{\mathfrak{T},n+1} - I_i^{\mathfrak{T},n+1}, \varphi_i^{\mathfrak{T}} \big]\!\big]_\Omega = 0,\\
\beta c_m \dfrac{1}{\Delta t} \big[\!\big[ v_1^{\mathfrak{T},n+1} - v_1^{\mathfrak{T},n}, \varphi_e^{\mathfrak{T}} \big]\!\big]_\Omega - \big\{\!\!\big\{ \mathbf{M}_i^{\mathfrak{T}} \nabla^{\mathfrak{T}} u_e^{\mathfrak{T},n+1}, \nabla^{\mathfrak{T}} \varphi_e^{\mathfrak{T}} \big\}\!\!\big\}_\Omega + \big[\!\big[ \beta I_{\text{ion}}^{\mathfrak{T},n+1} - I_e^{\mathfrak{T},n+1} - G^{\mathfrak{T},n+1}, \varphi_e^{\mathfrak{T}} \big]\!\big]_\Omega = 0,\\
-\big\{\!\!\big\{ \mathbf{M}_i^{\mathfrak{T}} \nabla^{\mathfrak{T}} u_s^{\mathfrak{T},n+1}, \nabla^{\mathfrak{T}} \varphi_s^{\mathfrak{T}} \big\}\!\!\big\}_\Omega - \big[\!\big[ I_s^{\mathfrak{T},n+1} + G^{\mathfrak{T},n+1}, \varphi_s^{\mathfrak{T}} \big]\!\big]_\Omega = 0,\\
\dfrac{1}{\Delta t} \big[\!\big[ w^{\mathfrak{T},n+1} - w^{\mathfrak{T},n}, \varphi^{\mathfrak{T}} \big]\!\big]_\Omega - \big[\!\big[ H^{\mathfrak{T},n+1}, \varphi^{\mathfrak{T}} \big]\!\big]_\Omega = 0.
\end{cases} \tag{4.3}$$

Notice that the equivalence of the formulations (4.1) and (4.3) is easy to establish. Now we parametrize our mesh by $h = \max\{\text{size}(\mathcal{T}), \Delta t\})$.

The convergence of the FV method given above is established by our main result, formulated as follows.

**Theorem 4.1.** *Suppose that $v_{1,0}, w_0 \in L^2(\Omega)$ and $I_j \in L^2(\Omega_T)$ for $j = i, e, s$. Then the FV solution $(u_i^{\mathfrak{T},\Delta t}, u_e^{\mathfrak{T},\Delta t}, u_s^{\mathfrak{T},\Delta t}, v_1^{\mathfrak{T},\Delta t}, v_2^{\mathfrak{T},\Delta t}, w^{\mathfrak{T},\Delta t})$, generated by* (4.1)–(4.2)*, converges along a subsequence to $\mathbf{u}$ as $h \to 0$, where $\mathbf{u} = (v_1, v_2, u_i, u_e, u_s, w)$ is a weak solution of* (1.1), (1.2), (1.3)*. The convergence is understood in the following sense*:

$$\begin{aligned}
&v_1^{\mathfrak{T},\Delta t} \to v_1 \quad \textit{strongly in } L^2(\Omega_T) \textit{ and a.e. in } \Omega_T,\\
&v_2^{\mathfrak{T},\Delta t} \to v_2 \quad \textit{weakly in } L^2(\Omega_T),\\
&\nabla^{\mathfrak{T}} u_j^{\mathfrak{T},\Delta t} \to \nabla u_j \quad \textit{weakly in } \big(L^2(\Omega_T)\big)^2 \quad \textit{for } j = i, e, s,\\
&w^{\mathfrak{T},\Delta t} \to w \quad \textit{weakly in } L^2(\Omega_T).
\end{aligned}$$

**Proof.** (Sketched.) *Well-definedness of the scheme*: Let $H^{\mathfrak{T}}(\Omega) \subset L^2(\Omega)$ be the space of piecewise constant functions on each $K \in \mathcal{T}$. For $(u^{\mathfrak{T}}, v^{\mathfrak{T}}) \in (H^{\mathfrak{T}}(\Omega))^2$, we define

$$\langle u^{\mathfrak{T}}, v^{\mathfrak{T}} \rangle_{H^{\mathfrak{T}}} := \big\{\!\!\big\{ \nabla^{\mathfrak{T}} u^{\mathfrak{T}}, \nabla^{\mathfrak{T}} v^{\mathfrak{T}} \big\}\!\!\big\}_\Omega, \qquad \|u^{\mathfrak{T}}\|_{H^{\mathfrak{T}}(\Omega)} := \big( \big\{\!\!\big\{ \nabla^{\mathfrak{T}} u^{\mathfrak{T}}, \nabla^{\mathfrak{T}} u^{\mathfrak{T}} \big\}\!\!\big\}_\Omega \big)^{1/2}.$$

We also define $L^{\mathfrak{T}}(\Omega) \subset L^2(\Omega)$ as the space of piecewise constant functions on each $K \in \mathcal{T}$ with the inner product and associated norm

$$\big(u^{\mathfrak{T}}, v^{\mathfrak{T}}\big)_{L^{\mathfrak{T}}(\Omega)} = \big[\!\big[ u^{\mathfrak{T}}, v^{\mathfrak{T}} \big]\!\big]_\Omega, \qquad \|u^{\mathfrak{T}}\|_{L^{\mathfrak{T}}(\Omega)} = \big( \big[\!\big[ u^{\mathfrak{T}}, u^{\mathfrak{T}} \big]\!\big]_\Omega \big)^{1/2}, \quad \text{for } u^{\mathfrak{T}}, v^{\mathfrak{T}} \in L^{\mathfrak{T}}(\Omega).$$

Let $E^{\mathfrak{T}} := H^{\mathfrak{T}}(\Omega) \times H^{\mathfrak{T}}(\Omega) \times H^{\mathfrak{T}}(\Omega) \times L^{\mathfrak{T}}(\Omega)$ be a Hilbert space endowed with the obvious norm, let $\mathbf{u}^{\mathfrak{T},\Delta t} = (u_i^{\mathfrak{T},\Delta t}, u_e^{\mathfrak{T},\Delta t}, u_s^{\mathfrak{T},\Delta t}, w^{\mathfrak{T},\Delta t})$ and $\Phi^{\mathfrak{T}} = (\varphi_i^{\mathfrak{T}}, \varphi_e^{\mathfrak{T}}, \varphi_s^{\mathfrak{T}}, \varphi^{\mathfrak{T}}) \in E^{\mathfrak{T}}$.

We now define the mapping $\mathcal{A} : E^{\mathfrak{T}} \to E^{\mathfrak{T}}$ by

$$\begin{aligned}
\left[\mathcal{A}\left(\mathbf{u}^{\mathfrak{T},\Delta t}\right), \Phi^{\mathfrak{T}}\right] = {} & \beta c_m \frac{1}{\Delta t} \left[\!\left[ v_1^{\mathfrak{T},n+1} - v_1^{\mathfrak{T},n}, \varphi_i^{\mathfrak{T}} \right]\!\right]_\Omega + \left\{\!\left\{ \mathbf{M}_i^{\mathfrak{T}} \nabla^{\mathfrak{T}} u_i^{\mathfrak{T},n+1}, \nabla^{\mathfrak{T}} \varphi_i^{\mathfrak{T}} \right\}\!\right\}_\Omega \\
& + \left[\!\left[ \beta I_{\mathrm{ion}}^{\mathfrak{T},n+1} - I_i^{\mathfrak{T},n+1}, \varphi_i^{\mathfrak{T}} \right]\!\right]_\Omega + \beta c_m \frac{1}{\Delta t} \left[\!\left[ v_1^{\mathfrak{T},n+1} - v_1^{\mathfrak{T},n}, \varphi_e^{\mathfrak{T}} \right]\!\right]_\Omega - \left\{\!\left\{ \mathbf{M}_i^{\mathfrak{T}} \nabla^{\mathfrak{T}} u_e^{\mathfrak{T},n+1}, \nabla^{\mathfrak{T}} \varphi_e^{\mathfrak{T}} \right\}\!\right\}_\Omega \\
& + \left[\!\left[ \beta I_{\mathrm{ion}}^{\mathfrak{T},n+1} - I_e^{\mathfrak{T},n+1} - G^{\mathfrak{T},n+1}, \varphi_e^{\mathfrak{T}} \right]\!\right]_\Omega - \left\{\!\left\{ \mathbf{M}_i^{\mathfrak{T}} \nabla^{\mathfrak{T}} u_s^{\mathfrak{T},n+1}, \nabla^{\mathfrak{T}} \varphi_s^{\mathfrak{T}} \right\}\!\right\}_\Omega \\
& - \left[\!\left[ I_s^{\mathfrak{T},n+1} + G^{\mathfrak{T},n+1}, \varphi_s^{\mathfrak{T}} \right]\!\right]_\Omega + \frac{1}{\Delta t} \left[\!\left[ w^{\mathfrak{T},n+1} - w^{\mathfrak{T},n}, \varphi^{\mathfrak{T}} \right]\!\right]_\Omega - \left[\!\left[ H^{\mathfrak{T},n+1}, \varphi^{\mathfrak{T}} \right]\!\right]_\Omega,
\end{aligned}$$

for all $\Phi^{\mathfrak{T}} \in E^{\mathfrak{T}}$. Using the discrete Hölder inequality, we then conclude that $\mathcal{A}$ is continuous and the task is now to show that

$$\left[\mathcal{A}\left(\mathbf{u}^{\mathfrak{T},n+1}\right), \mathbf{u}^{\mathfrak{T},n+1}\right] > 0 \quad \text{for } \left\|\mathbf{u}^{\mathfrak{T},n+1}\right\|_{E^{\mathfrak{T}}} = r > 0$$

for a sufficiently large $r$. But this can be done as in [8] so we omit the details. This concludes the proof of existence of at least one solution to (4.1) and (4.2).

*A priori estimates* (*estimates of the discrete solution*): We use (4.3) with $\varphi_i^{\mathfrak{T}} = u_i^{\mathfrak{T},n+1}$, $\varphi_e^{\mathfrak{T}} = -u_e^{\mathfrak{T},n+1}$, $\varphi_s^{\mathfrak{T}} = u_s^{\mathfrak{T},n+1}$ and $\varphi^{\mathfrak{T}} = w^{\mathfrak{T},n+1}$, and we sum over $n = 1, \ldots, k$ for all $1 < k \leqslant N$. The result is

$$\begin{aligned}
& \frac{1}{2} \beta c_m \left[\!\left[ v_1^{\mathfrak{T},k+1}, v_1^{\mathfrak{T},k+1} \right]\!\right]_\Omega + \frac{1}{2} \left[\!\left[ w^{\mathfrak{T},k+1}, w^{\mathfrak{T},k+1} \right]\!\right]_\Omega + \beta \int_0^{(k+1)\Delta t} \int_\Omega I_{\mathrm{ion}}^{\mathfrak{T},\Delta t} v_1^{\mathfrak{T},\Delta t} \\
& \quad + C_M \int_0^{(k+1)\Delta t} \int_\Omega \left( \left|\nabla^{\mathfrak{T}} u_i^{\mathfrak{T},\Delta t}\right|^2 + \left|\nabla^{\mathfrak{T}} u_e^{\mathfrak{T},\Delta t}\right|^2 + \left|\nabla^{\mathfrak{T}} u_s^{\mathfrak{T},\Delta t}\right|^2 \right) \\
& \quad \leqslant \frac{1}{2} \left[\!\left[ v_1^{\mathfrak{T},0}, v_1^{\mathfrak{T},0} \right]\!\right]_\Omega + \frac{1}{2} \left[\!\left[ w^{\mathfrak{T},0}, w^{\mathfrak{T},0} \right]\!\right]_\Omega + \sum_{j=i,e,s} \int_0^{(k+1)\Delta t} \int_\Omega I_j^{\mathfrak{T},\Delta t} u_j^{\mathfrak{T},\Delta t} \\
& \quad - \int_0^{(k+1)\Delta t} \int_\Omega G^{\mathfrak{T},\Delta t} v_2^{\mathfrak{T},\Delta t} + \int_0^{(k+1)\Delta t} \int_\Omega H^{\mathfrak{T},\Delta t} w^{\mathfrak{T},\Delta t}.
\end{aligned}$$

Herein, we have used the positivity of $\mathbf{M}_{i,e}^{\mathfrak{T}}$ and the convexity inequality $a(a-b) \geqslant \frac{1}{2}(a^2 - b^2)$. Using the Cauchy–Schwarz inequality and the discrete Gronwall inequality, yields: there exist constants $C_1, C_2, C_3 > 0$, depending on $\Omega$, $T$, $v_{1,0}$, $w_0$, $\alpha$, $I_i$, $I_e$ and $I_s$ such that:

$$\left\| v_1^{\mathfrak{T},\Delta t} \right\|_{L^\infty(0,T;L^2(\Omega))} \leqslant C_1, \tag{4.4}$$

$$\left\| v_1^{\mathfrak{T},\Delta t} \right\|_{L^4(Q_T)} \leqslant C_2,$$

$$\left\| u_j^{\mathfrak{T},\Delta t} \right\|_{L^2(Q_T)} + \left\| \nabla^{\mathfrak{T}} u_j^{\mathfrak{T},\Delta t} \right\|_{L^2(Q_T)} \leqslant C_3, \quad \text{for } j = i, e, s. \tag{4.5}$$

*Convergence of the scheme*: Before passing to the limit, we prove that the family $v_1^{\mathfrak{T},\Delta t}$ of discrete solutions is relatively compact in $L^1(Q_T)$. We first apply the following lemma (cf. [2]).

**Proposition 4.1.** *Let $(v^{\mathfrak{T}_h,\Delta t_h})_h \in (\mathbb{R}_0^{\mathfrak{T}_h})^{N_\Delta t_h}$ be a family of discrete functions on the cylinder $(0,T) \times \Omega$ corresponding to a family $(\Delta t_h)_h$ of time steps and to a family $(\mathfrak{T}_h)_h$ of FV meshes of $\Omega$ (we understand that $h \geqslant \mathrm{size}(\mathfrak{T}_h) + \Delta t_h$). Assume that $\sup_{h \in (0,h_{\max}]} \mathrm{reg}(\mathfrak{T}_h) < +\infty$, where $\mathrm{reg}(\mathfrak{T}_h)$ measures the regularity of $\mathfrak{T}_h$.*

*For each $h > 0$, assume that the discrete functions $v^{\mathfrak{T}_h,\Delta t_h}$ satisfy the discrete evolution equations*

$$\frac{v^{\mathfrak{T}_h,n+1} - v^{\mathfrak{T}_h,n}}{\Delta t} = \mathrm{div}^{\mathfrak{T}_h} \vec{\mathcal{M}}^{\mathfrak{T}_h,n+1} + f^{\mathfrak{T}_h,n+1} \quad \textit{for } n \in [0, N_h],$$

*with some initial data $v^{\mathfrak{T}_h,0} \in \mathbb{R}^{\mathfrak{T}_h}$, source terms $f^{\mathfrak{T}_h,\Delta t_h} \in (\mathbb{R}^{\mathfrak{T}_h})^{N_\Delta t_h}$ and discrete fields $\vec{\mathcal{M}}^{\mathfrak{T}_h,\Delta t_h} \in ((\mathbb{R}^2)^{\mathfrak{D}_h})^{N_\Delta t_h}$.*

*Assume that there is a constant M such that the following uniform $L^1((0,T)\times\Omega)$ estimates hold*:

$$\sum_{n=0}^{N_h}\Delta t\big(\|v^{\mathfrak{M}_h,n+1}\|_{L^1(\Omega)}+\|f^{\mathfrak{M}_h,n+1}\|_{L^1(\Omega)}+\|\vec{\mathcal{M}}^{\mathfrak{T}_h,n+1}\|_{L^1(\Omega)}\big)\leqslant M,$$

*and*

$$\sum_{n=0}^{N_h}\Delta t\|\nabla^{\mathfrak{T}_h}v^{\mathfrak{T}_h,n+1}\|_{L^1(\Omega)}\leqslant M.$$

*Assume that the family $(v^{\mathfrak{M}_h,0})_h$ is bounded in $L^1_{loc}(\Omega)$.*

*Then for any sequence $(h_i)_i$ converging to zero there exist $v\in L^1((0,T)\times\Omega)$ such that, extracting if necessary a sub-sequence,*

$$v^{\mathfrak{M}_{h_i},\Delta t_{h_i}}\longrightarrow v,\quad in\ L^1_{loc}\big((0,T)\times\Omega\big)\quad as\ i\to\infty.$$

Herein we define the mentioned norm (in Proposition 4.1) as

$$\|f^{\tau,\Delta t}\|_{L^p(0;T)}=\left(\sum_{n=0}^{N}\big|f^{\tau,n+1}\big|^p\right)^{1/p}\quad\text{for any function } f \text{ and } p\geqslant 1.$$

Note that as a consequence of Proposition 4.1 and (4.4)–(4.5), there exists a subsequence of $\mathbf{u}^{\mathfrak{T},\Delta t}=(u_i^{\mathfrak{T},\Delta t},u_e^{\mathfrak{T},\Delta t},u_s^{\mathfrak{T},\Delta t},v_1^{\mathfrak{T},\Delta t},v_2^{\mathfrak{T},\Delta t},w^{\mathfrak{T},\Delta t})$, not relabeled, such that, as $h\to 0$,

$$\begin{aligned}
&\text{(i) } \mathbf{u}^{\mathfrak{T},\Delta t}\to\mathbf{u}\quad\text{weakly in } L^1\big(\Omega_T,\mathbb{R}^6\big),\\
&\text{(ii) } u_j^{\mathfrak{T},\Delta t}\to u_j,\qquad \nabla^{\mathfrak{T}}u_j^{\mathfrak{T},\Delta t}\to\nabla u_j\quad\text{weakly in } L^2(Q),\quad\text{for } j=i,e,s,\\
&\text{(iii) } v_1^{\mathfrak{T},\Delta t}\to v_1\quad\text{strongly in } L^{4-\varepsilon}(Q_T),\quad\text{for all } \varepsilon>0,
\end{aligned}\tag{4.6}$$

where $\mathbf{u}=(v_1,v_2,u_i,u_e,u_s,w)$.

What is left to show is that the limit functions $v_1$, $v_2$, $u_i$, $u_e$, $u_s$, $w$ constructed in (4.6) actually constitute a weak solution of (1.1), (1.2), (1.3).

Let $\varphi_j,\phi\in D([0,T)\times\overline{\Omega})$ for $j=i,e,s$, then we use the discrete weak formulation (4.3) with test function $\Delta t\varphi_i^{\mathfrak{T},n+1}$ at time level $n$, and sum over $n$. What we get is

$$\begin{aligned}
&c_m\beta\sum_{n=0}^{N}\big[\!\big[v_1^{\mathfrak{T},n+1}-v_1^{\mathfrak{T},n},\varphi_i^{\mathfrak{T},n+1}\big]\!\big]_\Omega+\beta\sum_{n=0}^{N}\Delta t\big[\!\big[I_{\text{ion}}^{\mathfrak{T},n+1},\varphi_i^{\mathfrak{T},n+1}\big]\!\big]_\Omega+\sum_{n=0}^{N}\Delta t\big\{\!\!\big\{\mathbf{M}_i^{\mathfrak{T}}\nabla^{\mathfrak{T}}u_i^{\mathfrak{T},n+1},\nabla^{\mathfrak{T}}\varphi_i^{\mathfrak{T},n+1}\big\}\!\!\big\}_\Omega\\
&\quad=\sum_{n=0}^{N}\Delta t\big[\!\big[I_i^{\mathfrak{T},n+1},\varphi_i^{\mathfrak{T},n+1}\big]\!\big]_\Omega.
\end{aligned}$$

Performing integration by parts and using the Lipschitz continuity of $\partial_t\varphi$ and the definition of $v_{1,0}^{\mathfrak{T}}$, to get

$$\sum_{n=0}^{N}\big[\!\big[v_1^{\mathfrak{T},n+1}-v_1^{\mathfrak{T},n},\varphi_i^{\mathfrak{T},n+1}\big]\!\big]_\Omega=-\iint_{Q_T}v_1^{\mathfrak{T},\Delta t}\partial_t\varphi_i-\int_\Omega v_{1,0}\varphi_i(0,\cdot)+E^1_{\varphi_i}\big(\text{size}(\mathfrak{T}),\Delta t\big),$$

where the remainder term $E^1_{\varphi_i}$ is such that $E^1_{\varphi_i}(\text{size}(\mathfrak{T}),\Delta t)$ tends to zero as $\text{size}(\mathfrak{T})$ and $\Delta t$ tend to zero. Observe that

$$\begin{aligned}
\sum_{n=0}^{N}\Delta t\int_\Omega I_{\text{ion}}^{\mathfrak{T},n+1}\varphi_i^{\mathfrak{T},n+1}&=\iint_{Q_T}I_{\text{ion}}\big(v^{\mathfrak{T},\Delta t},w^{\mathfrak{T},\Delta t}\big)\varphi_i^{\mathfrak{T},\Delta t}\\
&=\iint_{Q_T}I_{\text{ion}}\big(v^{\mathfrak{T},\Delta t},w^{\mathfrak{T},\Delta t}\big)\varphi_i+E^2_{\varphi_i}\big(\text{size}(\mathfrak{T}),\Delta t\big),
\end{aligned}$$

and (because the discrete gradients are constant per diamond)

$$\sum_{n=0}^{N}\Delta t\int_\Omega\mathbf{M}_i^{\mathfrak{T}}\nabla^{\mathfrak{T}}u_i^{\mathfrak{T},n+1}\cdot\nabla\varphi_i^{\mathfrak{T},n+1}=\iint_{Q_T}\mathbf{M}_i(\cdot)\nabla^{\mathfrak{T}}u_i^{\mathfrak{T},\Delta t}\cdot\nabla\varphi_i+E^3_{\varphi_i}\big(\text{size}(\mathfrak{T}),\Delta t\big),$$

where $E^2_{\varphi_i}(\text{size}(\mathfrak{T}), \Delta t)$, $E^2_{\varphi_i}(\text{size}(\mathfrak{T}), \Delta t) \to 0$ as $\text{size}(\mathfrak{T}), \Delta t \to 0$. Similarly, thanks to further consistency results

$$\sum_{n=0}^{N} \Delta t \left[\!\left[ I_i^{\mathfrak{T},n+1}, \varphi_i^{\mathfrak{T},n+1} \right]\!\right]_\Omega = \iint\limits_{Q_T} I_i \varphi_i + E^4_{\phi_i}\big(\text{size}(\mathfrak{T}), \Delta t\big),$$

where $E^4_{\varphi_i}(\text{size}(\mathfrak{T}), \Delta t) \to 0$ as $\text{size}(\mathfrak{T}), \Delta t \to 0$. Gathering the above calculations, we arrive at:

$$\begin{aligned}
&\iint\limits_{Q_T} \big(-v_1^{\mathfrak{T},\Delta t} \partial_t \varphi_i + \mathbf{M}_i(\cdot) \nabla^{\mathfrak{T}} u_i^{\mathfrak{T},\Delta t} \cdot \nabla \varphi_i + I_{\text{ion}}\big(v^{\mathfrak{T},\Delta t} \varphi_i\big) \\
&\quad = \int\limits_\Omega v_{1,0}\, \varphi(0,\cdot) + \iint\limits_{Q_T} I_i \varphi_i + E^1_{\varphi_i}\big(\text{size}(\mathfrak{T}), \Delta t\big) + E^2_{\varphi_i}\big(\text{size}(\mathfrak{T}), \Delta t\big) \\
&\qquad + E^3_{\varphi_i}\big(\text{size}(\mathfrak{T}), \Delta t\big) + E^4_{\varphi_i}\big(\text{size}(\mathfrak{T}), \Delta t\big).
\end{aligned} \tag{4.7}$$

Reasoning along the same lines as above, we conclude that also (4.7) holds for $u_e^{\mathfrak{T},\Delta t}$, $u_s^{\mathfrak{T},\Delta t}$ and $w^{\mathfrak{T},\Delta t}$.

Finally, in view of (4.6) and (4.7), we conclude that the limit $\mathbf{u} = (v_1, v_2, u_i, u_e, u_s, w)$ of $\mathbf{u}^{\mathfrak{T},\Delta t} = (u_i^{\mathfrak{T},\Delta t}, u_e^{\mathfrak{T},\Delta t}, u_s^{\mathfrak{T},\Delta t}, v_1^{\mathfrak{T},\Delta t}, v_2^{\mathfrak{T},\Delta t}, w^{\mathfrak{T},\Delta t})$ is a weak solution of (1.1)–(1.3). □

## 5. The minimization procedure

The optimization stage at the discrete level is carried out using the well known nonlinear conjugate gradient method (see e.g. [15]). Other alternatives, such as second order algorithms, are certainly feasible (see e.g. [18]), but we stick to the fairly simple present setting.

As mentioned in Section 1, here we consider the "optimize-then-discretize" approach, and at each iteration of the minimization procedure, the method requires the solution of the discrete state and adjoint equations. The discrete state equations can be solved by marching forward in time starting from the initial conditions (1.3), while the discrete adjoint equations can be solved by marching backward in time starting from the terminal conditions (3.4). Other alternatives such as the *one shot* strategy have been proposed to obtain the solution of both forward and backward problems monolithically, but we leave those for a future work. As pointed out in Section 3, the cost functional is minimized with respect to $v_1$ in $\Omega_o$ and $I_s$ in $\Omega_c$.

To compute the optimal control, we improve the initial guess $I_s^0$ by using the Jacobian of the reduced objective $\hat{J}^k$ in the direction $d^k = -\nabla \hat{J}^k$, the latter being also updated at each iteration step, according to the rule $d^{k+1} = -\nabla \hat{J}^k + \varrho^k d^k$, where the sequence $\{\varrho^k\}_k$, is computed using the Hestenes–Stiefel formula [17]

$$\varrho^k = \frac{(\nabla \hat{J}^{k+1}, \nabla \hat{J}^{k+1} - \nabla \hat{J}^k)_{L^2}}{(d^{k-1}, \nabla \hat{J}^{k+1} - \nabla \hat{J}^k)_{L^2}}. \tag{5.1}$$

The scaling for the updating of the control at step $k$ is given by $\delta^k$, which is updated following Armijo's rule, i.e., it is reduced by the half until the first Wolfe condition

$$\hat{J}\big(I_s^k + \delta^k d^k\big) \leqslant \hat{J}^k + \alpha d^k \nabla \hat{J}^k$$

is satisfied.

Before presenting our numerical examples, we provide a formal description of the overall solution algorithm.

**Algorithm 1.** Overall solution algorithm.

set initial value for the tolerances $\alpha_{abs}$, $\alpha_{rel}$
set $k = 0$, $\delta^0$ and $\varrho^0$
set initial guess $I_s^0$ for the control variable $I_s$
**for** $k = 1, \dots, \max\_outer\_iterations$ **do**
  **for** $t = t^1, \dots, t^{total\_time\_steps}$ **do**
    Compute $(v_1, u_e, u_s, w)$ from the state Eqs. (1.1)
  **end for**
  Evaluate the reduced cost functional $\hat{J}^k$.
  **for** $t = t^{total\_time\_steps}, \dots, t^1$ **do**
    Being known the state variables $(v_1, u_e, u_s, w)$, compute the solution $(p_1, p_e, p_s, q)$ of the adjoint problem (3.3).
  **end for**
  Compute the Jacobian $\nabla \hat{J}^k$.
  **if** $\|\nabla \hat{J}^k\|_{L^2} \leqslant \alpha_{rel} \|\nabla \hat{J}^0\|_{L^2}$ **and** $\|\nabla \hat{J}^k\|_{L^2} \leqslant \alpha_{abs}$ **then**

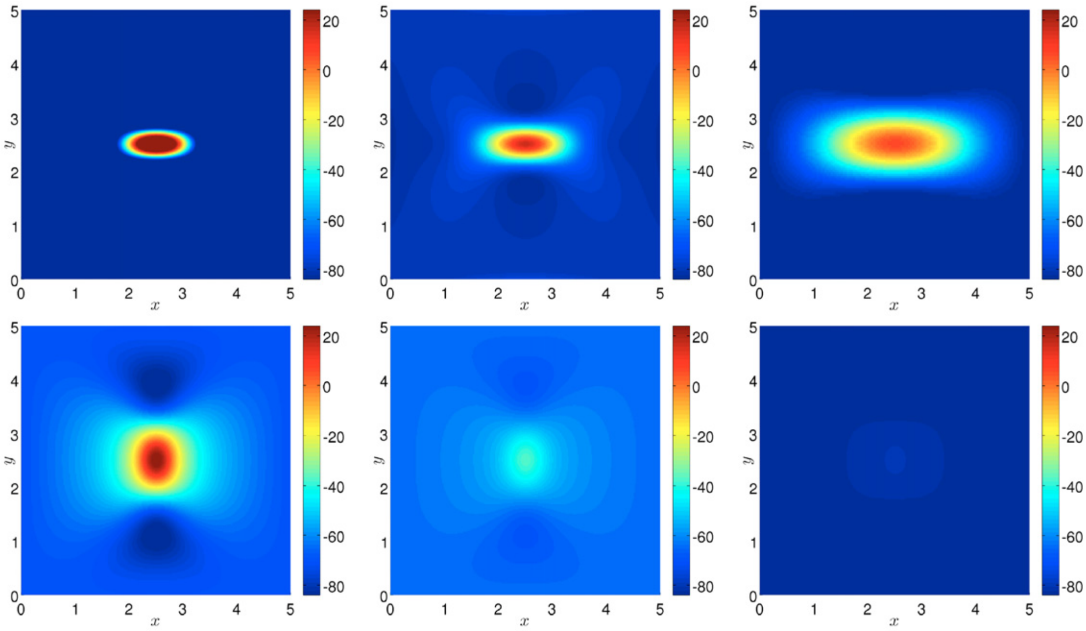


**Fig. 3.** Uncontrolled (top) and controlled (bottom) numerical solution for $v_1$ at time instants $t = 1$ ms (left), $t = 20$ ms (middle) and $t = 60$ ms (right).

    break
  **else**
    Compute step length $\delta^k > 0$
    Update the value of the control variable $I_s^{k+1} = I_s^k + \delta^k d^k$
    Compute the step $\varrho^k$ from (5.1)
    Update the direction $d^{k+1} = -\nabla \hat{J}^k + \varrho^k d^k$
  **end if**
**end for**

## 6. Numerical results

This section is devoted to the presentation of numerical tests to validate the algorithm introduced in the previous section. The state and adjoint equations are discretized using a backward and forward Euler schemes in time, respectively. That is, at each iteration of the gradient algorithm, we sequentially solve the state problem by marching forward in time, whereas the adjoint problem is solved by marching backwards in time starting from terminal conditions. Even in the case of a simple square domain, the multi-query nature of the optimal control procedure is computationally demanding. This is even more severe in the case of a time-dependent problem. In our particular case, the wall-time to perform a full simulation is of about 4 hours (on a four-cores workstation of 16 GB RAM). The particular choice of numerical and optimization parameters essentially follows [25,26].

We employ the observation and control domains $\Omega_c = B_{0.2}(2.5, 2.5)$, $\Omega_c = B_{0.2}(2.5, 4) \cup B_{0.2}(2.5, 1)$, where $B_r(x, y)$ denotes the ball of radius $r$ centered on $(x, y)$. The computational spatial domain is $\Omega = (0, 5)^2$, the final simulated time is $T = 60\,\text{ms}$, the regularization parameter is $\alpha = 10^{-4}$ (a justification is provided at the end of this section). The spatial domain is discretized with rectangular control volumes of size $h = 0.0049$, and the time interval is discretized uniformly with stepsize $\Delta t = 5 \times 10^{-4}$. The initial guess for the control variable is $I_s^0(x, t) = 0$, for $x \in \Omega$.

From Figs. 3, 4 (the difference being the initial data) we can observe the evolution history of the transmembrane potential $v_1$, when the control is switched on/off. The uncontrolled solution is obtained by setting $I_s$ constant in time. Notice that for the uncontrolled system, by advancing in time, the raise in the transmembrane potential propagates from the inside to the outside of the computational domain, whereas for the optimally controlled case, almost all of the wave propagation has been successfully damped. The decay of the reduced cost functional along the minimization process is depicted in Fig. 5, where the minimum of $\hat{J}^k$ is plotted versus the iteration count $k$. We observe that the major contribution to $\hat{J}^k$ is carried by the term $\int_0^T \int_\Omega |v_1|^2$ in almost all of the iteration process.

Fig. 6 displays the optimally controlled stimulus $I_s(\bar{x}, \cdot)$ over the time evolution, at a fixed position in the control domain for different values of the absolute stopping criterion. In addition, to assess the importance of the regularization parameter $\alpha$ of the cost functional, in Table 1 we depict the minimum of $\hat{J}^k$ and the quantity $\|\nabla \hat{J}^k\|_{L^2}$ during the optimization iteration, for different values of $\alpha$. In the light of the middle column, we confirm that a suitable value is $\alpha = 10^{-4}$, since

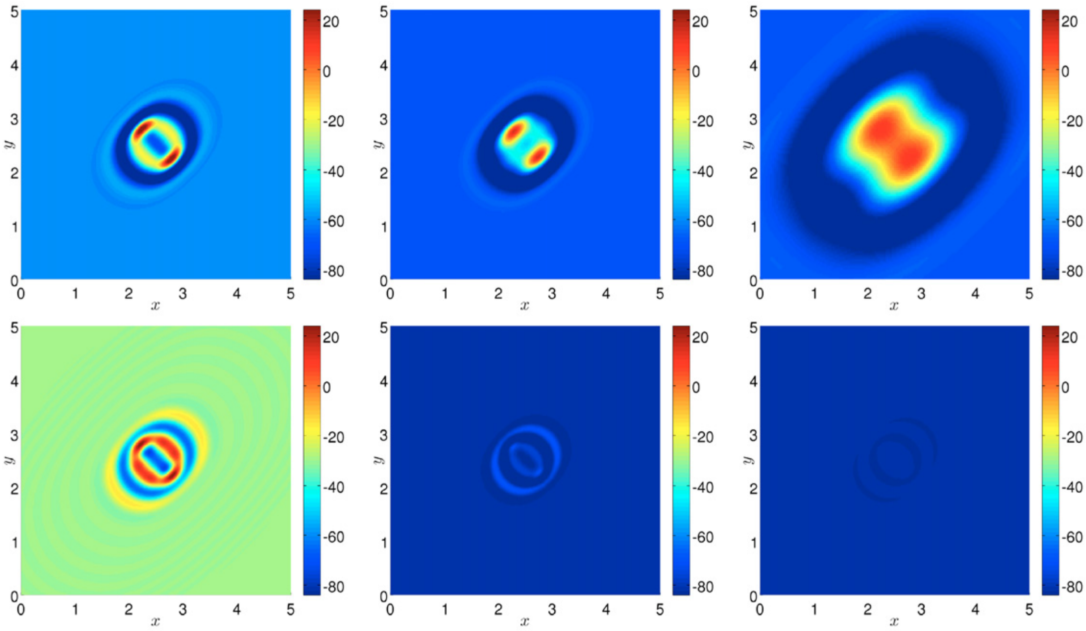


**Fig. 4.** Uncontrolled (top) and controlled (bottom) numerical solution for $v_1$ at time instants $t = 1$ ms (left), $t = 20$ ms (middle) and $t = 60$ ms (right).

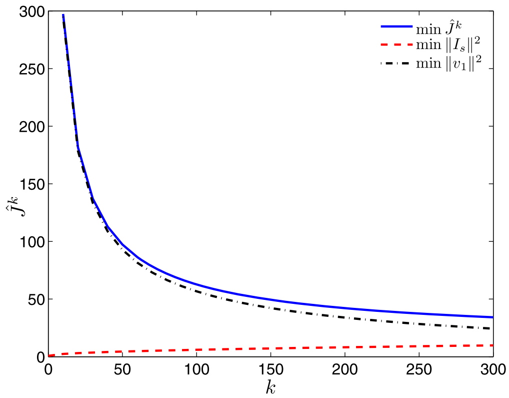


**Fig. 5.** Minimum over $\Omega_T$ of the reduced cost functional $\hat{J}^k$ at each optimization step. The final simulated time is $T = 60$ ms.

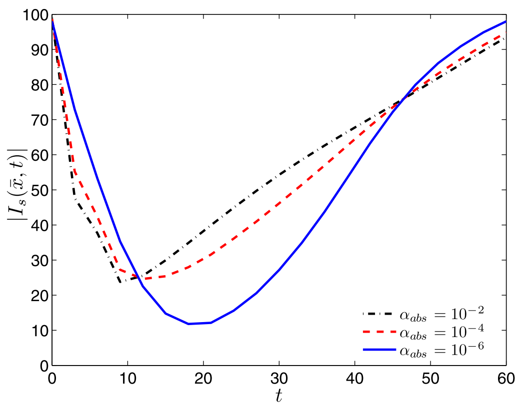


**Fig. 6.** Time evolution of the optimized applied stimulus $I_s$ at a fixed spatial position $\bar{x} \in \Omega_c$ for different values of $\alpha_{abs}$.

**Table 1**
Reduced cost functional and norm of the residual versus the outer iteration count for different values of the regularization parameter $\alpha$. The simulated final time is $T = 5$ ms.

| $\alpha$ | $k$ | $\min \hat{J}^k$ | $\|\nabla \hat{J}^k\|_{L^2(\Omega)}$ |
|---|---|---|---|
| $10^{-3}$ | 10 | 315.3821 | $5.8238 \times 10^{+1}$ |
| | 50 | 256.1845 | $1.4267 \times 10^{+1}$ |
| | 100 | 130.1330 | $8.7129 \times 10^{-1}$ |
| | 150 | 26.7982 | $2.5613 \times 10^{-2}$ |
| $10^{-4}$ | 10 | 287.3927 | $1.6211 \times 10^{+1}$ |
| | 50 | 192.6411 | $1.4013 \times 10^{+0}$ |
| | 100 | 79.7086 | $5.5109 \times 10^{-2}$ |
| | 150 | 6.3394 | $2.3448 \times 10^{-4}$ |
| $10^{-5}$ | 10 | 265.4125 | $7.6516 \times 10^{+0}$ |
| | 50 | 180.9871 | $4.5301 \times 10^{-1}$ |
| | 100 | 76.3224 | $6.2259 \times 10^{-3}$ |
| | 150 | 1.6763 | $8.2458 \times 10^{-5}$ |

with $\alpha = 10^{-5}$ the gain in the minimization of the reduced cost is not substantial whereas the overall computation is more computationally expensive. Moreover, from the right column we notice that the quadratic rate of convergence is already achieved from the iteration count $k = 50$ for the values $\alpha = 10^{-4}$ and $\alpha = 10^{-5}$.

## 7. Conclusion

In this paper, we presented a finite volume scheme for the numerical solution of an optimal control problem related to the tridomain equations in cardiac electrophysiology, when an external bath is considered in the model. The wellposedness analysis of the continuous problem is performed and the convergence of the numerical scheme is addressed in detail. Existence of the optimal solution and first order optimality conditions were discussed as well.

Our preliminary numerical results obtained with the aid of a finite volume formulation, are satisfactory in qualitatively assessing the proper mechanisms for low-voltage defibrillation. We hope that the compound of the mathematical problem and our results could provide more insights into the field situation. However, several improvements are envisaged from the numerical standpoint. First, a second order method such as Newton-CG will be useful to reduce the computational cost. Other possible extensions include space [7] and time adaptive strategies, discrete gradient projection methods and model order reduction techniques (see e.g. [14,31]).

From the mathematical and numerical viewpoint, the extension to the 3D case is straightforward, however at the modeling stage (even when a forward problem related to (1.1) has been solved in [3]), the importance of considering a bidomain model in an external bath as part of the homogenized superimposed medium, is not yet well established in the literature. This is why our following related study will address an inverse problem considering the external bath as a different domain at the macroscale. A further application deals with studying the importance of considering an external bath not only as a passive conductor, but also as a way of introducing physiologically relevant mechanical boundary data for electromechanical cardiac models (see e.g. [28]). Nevertheless, these topics are beyond the scope of this paper and will be discussed in more detail in a forthcoming contribution.

## Acknowledgments

RR acknowledges financial support by the European Research Council through the Advanced Grant *Mathcard, Mathematical Modelling and Simulation of the Cardiovascular System*, Project ERC-2008-AdG 227058. This work started during a visit of RR to the Institut de Mathématiques de Bordeaux, Université Victor Segalen Bordeaux 2 (Bordeaux, France).

## References

[1] B. Andreianov, M. Bendahmane, K.H. Karlsen, Discrete duality finite volume schemes for doubly nonlinear degenerate hyperbolic–parabolic equations, J. Hyperbolic Differ. Equ. 7 (2010) 1–67.
[2] B. Andreianov, M. Bendahmane, R. Ruiz-Baier, Analysis of a finite volume method for a cross-diffusion model in population dynamics, M3AS Math. Models Methods Appl. Sci. 21 (2011) 307–344.
[3] O.V. Aslanidi, A.P. Benson, M.R. Boyett, H. Zhang, Mechanisms of defibrillation by standing waves in the bidomain ventricular tissue with voltage applied in an external bath, Phys. D 238 (2009) 984–991.
[4] M.E. Belik, T.P. Usyk, A.D. McCulloch, Computational methods for cardiac electrophysiology, in: N. Ayache (Ed.), Computational Models for the Human Body, Handbook of Numerical Analysis, Elsevier, North-Holland, 2004, pp. 129–187.
[5] M. Bendahmane, K.H. Karlsen, Analysis of a class of degenerate reaction–diffusion systems and the bidomain model of cardiac tissue, Netw. Heterog. Media 1 (2006) 185–218.
[6] M. Bendahmane, K.H. Karlsen, Convergence of a finite volume scheme for the bidomain model of cardiac tissue, Appl. Numer. Math. 59 (2009) 2266–2284.
[7] M. Bendahmane, R. Bürger, R. Ruiz-Baier, A multiresolution space-time adaptive scheme for the bidomain model in electrocardiology, Numer. Methods Partial Differential Equations 26 (2010) 1377–1404.
[8] M. Bendahmane, R. Bürger, R. Ruiz-Baier, A finite volume scheme for cardiac propagation in media with isotropic conductivities, Math. Comput. Simulation 80 (2010) 1821–1840.

[9] Y. Bourgault, Y. Coudière, C. Pierre, Existence and uniqueness of the solution for the bidomain model used in cardiac electro-physiology, Nonlinear Anal. Real World Appl. 10 (2009) 458–482.
[10] P. Colli Franzone, G. Savaré, Degenerate evolution systems modeling the cardiac electric field at micro- and macroscopic level, in: A. Lorenzi, B. Ruf (Eds.), Evolution Equations, Semigroups and Functional Analysis, Birkhäuser, Basel, 2002, pp. 49–78.
[11] Y. Coudière, C. Pierre, O. Rousseau, R. Turpault, 2D/3D discrete duality finite volume scheme (DDFV) applied to ECG simulation, in: R. Eymard, J.M. Herard (Eds.), Finite Volumes for Complex Applications (V), Wiley, 2008, pp. 313–320.
[12] R.W. Dos Santos, F. Dickstein, On the influence of a volume conductor on the orientation of currents in a thin cardiac tissue, in: Lecture Notes in Comput. Sci., vol. 2674, New York, 2003, pp. 111–121.
[13] R. FitzHugh, Impulses and physiological states in theoretical models of nerve membrane, Biophys. J. 1 (1961) 445–465.
[14] B. Haasdonk, M. Ohlberger, Reduced basis method for finite volume approximations of parametrized linear evolution equations, M2AN Math. Model. Numer. Anal. 42 (2008) 277–302.
[15] W.W. Hager, H. Zhang, A survey of nonlinear conjugate gradient methods, Pac. J. Optim. 2 (2006) 35–58.
[16] F. Hermeline, Approximation of 2D and 3D diffusion operators with discontinuous full-tensor coefficients on arbitrary meshes, Comput. Methods Appl. Mech. Engrg. 196 (2007) 2497–2526.
[17] M.R. Hestenes, E.L. Stiefel, Methods of conjugate gradients for solving linear systems, J. Research Nat. Bur. Standards 49 (1952) 409–436.
[18] M. Hinze, K. Kunisch, Second order methods for optimal control of time-dependent fluid flow, SIAM J. Control Optim. 40 (2001) 925–946.
[19] M. Hinze, R. Pinnau, M. Ulbrich, S. Ulbrich, Optimization with PDE Constraints, Math. Model. Theory Appl., vol. 23, Springer, Netherlands, 2009.
[20] J. Keener, J. Sneyd, Mathematical Physiology, vols. I and II, second ed., Springer, New York, 2009.
[21] R. Kelly, A. Staines, R. MacWalter, P. Stonebridge, H. Tunstall-Pedoe, A.D. Struthers, The prevalence of treatable left ventricular systolic dysfunction in patients who present with noncardiac vascular episodes: A case-control study, J. Am. Coll. Cardiol. 39 (2002) 219–224.
[22] K. Kunisch, M. Wagner, Optimal control of the bidomain system (I): The monodomain approximation with the Rogers–McCulloch model, Nonlinear Anal. Real World Appl., in press.
[23] K. Kunisch, M. Wagner, Optimal control of the bidomain system (II): Uniqueness and regularity theorems for weak solutions, SFB Report, Graz University, 2011.
[24] J.L. Lions, Optimal Control of Systems Governed by Partial Differential Equations, Springer-Verlag, Berlin, 1971.
[25] C. Nagaiah, K. Kunisch, G. Plank, Numerical solution for optimal control of the reaction–diffusion equations in cardiac electrophysiology, Comput. Optim. Appl. 49 (2011) 149–178.
[26] C. Nagaiah, K. Kunisch, Adaptive and higher order numerical solution for optimal control of monodomain equations in cardiac electrophysiology, Appl. Numer. Math. 61 (2011) 53–65.
[27] J.S. Nagumo, S. Arimoto, S. Yoshizawa, An active pulse transmission line simulating nerve axon, Proc. Inst. Radio Eng. 50 (1962) 2061–2071.
[28] F. Nobile, A. Quarteroni, R. Ruiz-Baier, An active strain electromechanical model for cardiac tissue, Int. J. Numer. Meth. Biomed. Engrg., doi:10.1002/cnm.1468, in press.
[29] S. Sanfelici, Convergence of the Galerkin approximation of a degenerate evolution problem in electrocardiology, Numer. Methods Partial Differential Equations 18 (2002) 218–240.
[30] J. Sundnes, G.T. Lines, X. Cai, B.F. Nielsen, K.-A. Mardal, A. Tveito, Computing the Electrical Activity in the Heart, Springer-Verlag, Berlin, 2006.
[31] F. Tubino, G. Solari, Double proper orthogonal decomposition for representing and simulating turbulence fields, J. Engrg. Mech. 131 (2005) 1302.
[32] M. Veneroni, Reaction-diffusion systems for the macroscopic bidomain model of the cardiac electric field, Nonlinear Anal. Real World Appl. 10 (2009) 849–868.
[33] S. Volkwein, Nonlinear conjugate gradient methods for the optimal control of laser surface hardening, Optim. Methods Softw. 19 (2004) 179–199.
[34] E. Zuazua, Controllability and observability of partial differential equations: Some results and open problems, in: Handbook of Differential Equations: Evolutionary Equations, vol. III, North-Holland, Amsterdam, 2007, pp. 527–621.